
A Scalable and Effective Alternative to Graph Transformers

Kaan Sancak^{*†}
balin@gatech.edu

Zhigang Hua[‡]
zhua@meta.com

Jin Fang[†]
fangjin@meta.com

Yan Xie[†]
yanxie@meta.com

Andrey Malevich[†]
amelevich@meta.com

Bo Long[†]
bolong@meta.com

Muhammed Fatih Balin^{*}
balin@gatech.edu

Ümit V. Çatalyürek^{§*}
umit@gatech.edu

Abstract

Graph Neural Networks (GNNs) have shown impressive performance in graph representation learning, but they face challenges in capturing long-range dependencies due to their limited expressive power. To address this, Graph Transformers (GTs) were introduced, utilizing self-attention mechanism to effectively model pairwise node relationships. Despite their advantages, GTs suffer from quadratic complexity w.r.t. the number of nodes in the graph, hindering their applicability to large graphs. In this work, we present Graph-Enhanced Contextual Operator (GECO), a scalable and effective alternative to GTs that leverages neighborhood propagation and global convolutions to effectively capture local and global dependencies in quasilinear time. Our study on synthetic datasets reveals that GECO reaches 169× speedup on a graph with 2M nodes w.r.t. optimized attention. Further evaluations on diverse range of benchmarks showcase that GECO scales to large graphs where traditional GTs often face memory and time limitations. Notably, GECO consistently achieves comparable or superior quality compared to baselines, improving the SOTA up to 4.5%, and offering a scalable and effective solution for large-scale graph learning.

1 Introduction

Graph Neural Networks (GNNs) have been state-of-the-art (SOTA) models for graph representation learning showing superior quality across different tasks spanning node, link, and graph level prediction [1, 2, 3, 4, 5]. Despite their success, GNNs have fundamental limitations that affect their ability to capture long-range dependencies in graphs. These dependencies refer to nodes needing to exchange information over long distances effectively, especially when the distribution of edges is not directly related to the task or when there are missing edges in the graph [6]. This limitation can further lead to information over-squashing caused by repeated propagations within GNNs [7, 8, 9].

Graph Transformers (GTs) [10, 11, 12] were introduced to overcome the limitations of GNNs by incorporating the self-attention mechanism [13], and achieved SOTA across various benchmarks. GTs can model long-range dependencies by attending to potential neighbors among the entire set of

^{*}School of Computational Science and Engineering, Georgia Institute of Technology, Atlanta, GA, USA

[†]This work was partially done when the first author was a research scientist intern at Meta AI.

[‡]Meta AI

[§]Amazon Web Services. This publication describes work performed at the Georgia Institute of Technology and is not associated with AWS.

nodes. However, GTs suffer from quadratic complexity in contrast to the linear time and memory complexity inherent in GNNs. This quadratic complexity stems from that each node needs to attend to every other node, preventing GTs’ widespread adoption in large-scale real-world scenarios. As mini-batch sampling methods for GTs remain under-explored, the primary application of GTs has been on smaller datasets, such as molecular ones [14, 15, 6, 16]. Consequently, exploring novel efficient and high-quality attention replacements remains a crucial research direction to unlock the full potential of GTs for large-scale graphs. Recently, global convolutional language models have emerged as promising alternatives for attention [17, 18]. Specifically, Hyena [19] has demonstrated impressive performance, offering efficient processing of longer contexts with high quality.

In this work, we aim to find an efficient alternative to dense attention mechanisms to scale graph transformers without sacrificing the modeling quality. The key challenge lies in designing an efficient model that can effectively capture both local and long-range dependencies within large graphs. To address this, we propose a novel compact layer called Graph-Enhanced Contextual Operator (GECO), which combines local propagations and global convolutions. The convolution filters in GECO encompass all nodes, serving as a substitute for dense attention in the graph domain. GECO consists of four main components: (1) local propagation to capture local context, (2) global convolution to capture global context with quasilinear complexity, (3) data-controlled gating for context-specific operations on each node, and (4) positional/structural encoder for feature encoding and graph ordering.

Our evaluation has two main objectives: **(O1)**: Matching SOTA GT quality on small graph datasets emphasized by the community. **(O2)**: Scaling to larger graphs where traditional attention mechanisms are impractical due to computational constraints. Extensive evaluations across diverse benchmarks of varying tasks and sizes demonstrate that GECO scales to larger datasets and consistently delivers strong quality, often achieving SOTA or competitive results. The main contributions of work include:

- We developed GECO, a compact layer consisting of local and global context blocks with quasilinear time complexity. Unlike prior work, GECO is a refined layer without intermediate parameters and non-linearities between local and global blocks, applying skip connections to the layer as a whole.
- To our knowledge, GECO is the first to employ a global convolution model to develop a scalable and effective alternative to self-attention based GTs. Notably, it improves computational efficiency while preserving prediction quality, and in most cases, it leads to improvements.
- We demonstrated that GECO scales to large-scale graphs that are infeasible for existing GTs utilizing self-attention due to their intrinsic quadratic complexity. GECO further enhances prediction accuracy by up to 4.5% for large graph datasets.
- We demonstrated GECO’s ability to capture long-range dependencies in graphs, achieving SOTA on the majority of long-range graph benchmark and improving results by up to 4.3%.

2 Background and Related Work

2.1 Graph Neural Networks (GNNs)

A graph $G = (V, E)$ comprises a set of vertices V and edges $E \subseteq V \times V$. $A \in \mathbb{R}^{N \times N}$ is the adjacency matrix and a weighted edge $(u \rightarrow v) \subseteq E$ exists between source u and target v if $A_{u,v} \neq 0$. The node feature matrix $X^{(0)} \in \mathbb{R}^{N \times d^{(0)}}$ maps v to a feature vector $x_v^{(0)} \in \mathbb{R}^{d^{(0)}}$. $\mathcal{N}(v) = \{u \mid (u \rightarrow v) \in E\}$ is the incoming neighbors of v . GNNs adopt an Aggregate-Combine framework [20] to compute layer- l representation $h_v^{(l)}$ such that:

$$h_v^{(l)} = \text{Combine}^{(l)}(\alpha_v^{(l)}, h_v^{(l-1)}), \quad \alpha_v^{(l)} = \text{Aggregate}^{(l)}(\{h_u^{(l-1)} : u \in \mathcal{N}(v)\}) \quad (1)$$

Additionally, a pooling function generates graph representation, $h_G = \text{Pool}(\{h_v^{(L)} \mid v \in V\})$.

Challenges. GNNs efficiently scale to large graphs with linear complexity, $\mathcal{O}(|V| + |E|)$, but they struggle with capturing long-range dependencies, often requiring many hops and nonlinearities for information to traverse distant nodes [8, 6]. GTs effectively resolve this via dense pairwise attention.

2.2 Graph Transformers (GTs)

Graph Transformers (GTs) generalize Transformers [13] to graphs. At the core of Transformer lies the multi-head self-attention (MHA) [13], which maps the input $H \in \mathbb{R}^{N \times d}$ to $\mathbb{R}^{N \times d}$ as:

$$\text{Attn}(H) = \text{Softmax} \left(\frac{QK^T}{\sqrt{d}} \right), \quad y = \text{SelfAttention}(H) = \text{Attn}(H)V \quad (2)$$

here *query* ($Q = HW_q$), *key* ($K = HW_k$), and *value* ($V = HW_v$) are linear projections of the input, $W_q, W_k, W_v \in \mathbb{R}^{d \times d}$. The attention matrix $\text{Attn}(H)$ captures the pair-wise similarities of the input.

Based on their *focus of attention*, we group GTs into three: **Sparse GTs** use the adjacency matrix as an attention mask, allowing nodes to pay attention to *their neighbors*, which facilitates weighted neighborhood aggregation [21, 22]. **Layer GTs** use a GNN to generate hop-tokens, followed by MHA on these tokens, where nodes pay attention to *their layer embeddings* [23, 24]. While both Sparse and Layer GTs use attention, they still struggle with long-range dependencies as their attention is restricted to fixed number of hops. Comparatively, **Dense GTs** use attention on fully connected graph, enabling nodes to pay attention to *all the other nodes* regardless of their distances. Various works have incorporated positional encodings (PE) into GTs to provide topological information to otherwise graph-unaware models [10, 25, 11, 26, 27, 28]. See Appendix E.1 for related work details.

Challenges. Dense GTs introduce computational and memory bottlenecks due to their increased complexity from $\mathcal{O}(|V| + |E|)$ to $\mathcal{O}(|V|^2)$, restricting their application to large graphs. GraphGPS [29] offers a modular framework that combines GNNs with a global attention module, including subquadratic Transformer approximations [30, 25]. Unfortunately, the subquadratic models compromise quality while MHA based ones struggle with scalability. Therefore, finding a subquadratic attention replacement with a good quality remains a challenge, and our work is dedicated to tackle this problem.

Other Related Work. Expformer [31] enhances GraphGPS by using attention on expander graphs. [32] generalizes ViT [33] and MLP-Mixer [34] to graphs. [35] formulates an adversary bandit problem to sample nodes. HSGT [36] learns multi-level hierarchies via coarsening. GOAT [37] uses dimensionality reduction to reduce computational cost of MHA. [38] utilizes additional edge updates.

2.3 Attention Alternatives

Consider an input u of length N and a filter z . A circular convolution can be computed at each position t of the input u , ranging from 0 to $N - 1$, as follows:

$$y_t = (u * z)_t = \sum_{i=0}^{N-1} u_i z_{(t-i) \bmod N} \quad (3)$$

where we assume a single-channel input and filter, which can be easily extended to multi-channel inputs. CNNs [39] optimize z_t at every K steps, where K is a fixed filter size. This *explicit* parametrization captures local patterns within every K steps. Alternatively, *implicit* parameterizations represent the filter as a learnable function [40, 41, 17, 42, 43, 44]. Convolutions can be efficiently computed through Fast Fourier Transform (FFT) in quasilinear time, offering a significant advantage.

A convolution is referred to as a global convolution when the filter has the same length as the input. Global convolutional models have demonstrated the ability to capture longer contexts through pairwise interactions (dot products) at any input position by proper filter parametrization, offering a promising alternative to attention [41, 17, 18]. Recently, Hyena [19] proposed a sequence model that combines short explicit convolutions and global implicit convolutions using a similar global filter design as CKConv and SGConv [17, 18], and it stands out by matching Transformer’s quality in quasilinear time. Please refer to Appendix C for details. However, to the best of our knowledge, there has been no prior work dedicated to designing and utilizing global convolutional models for graphs.

3 Proposed Architecture: GECO

We present Graph-Enhanced Contextual Operator (GECO), a novel compact layer developed to replace dense attention with quasilinear time and memory complexity. It draws inspiration from recent advancements in global convolutional models and offers a promising approach to capture local and

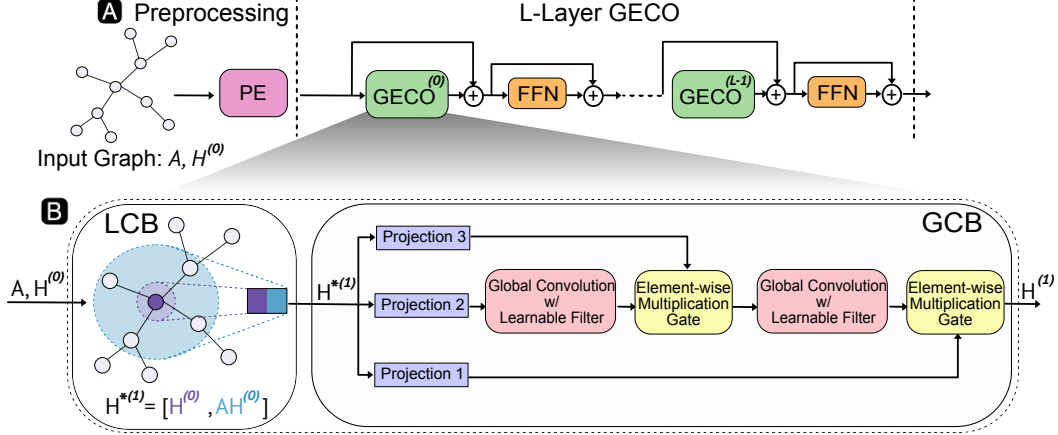


Figure 1: **A** Our architecture comprises Positional Encoding (PE) block and Graph-Enhanced Contextual Operators (GECOs) layers. PE adds positional encodings as a preprocessing step and each GECO is followed by an FFN. **B** A GECO layer contains a Local Propagation Block (LCB) aggregating neighborhood embeddings and concatenating with originals to capture local dependencies, and a Global Context Block (GCB) efficiently capturing global dependencies via global convolutions.

global dependencies with subquadratic operators. Unlike Hyena, which focuses on sequences, GECO is designed for graphs, combining local propagations with global convolutions. By utilizing the topological information of the adjacency matrix, it effectively captures local dependencies. Furthermore, it introduces a new global convolution filter design for graphs to capture global dependencies.

As illustrated in Figure 1, GECO starts with positional/structural encodings and proceeds through multiple layers of GECO, each followed by a feed-forward neural network (FFN). We introduce the main components in the following subsections.

3.1 Graph Structural/Positional Encodings

Structural and positional encodings play a pivotal role in the realm of graph transformers. In our approach, we follow the foundational work established in prior literature concerning these encodings [10, 25, 11, 45]. To seamlessly integrate these encodings with the original input features, we employ a concatenation method. Given a positional/structural encoding matrix $U \in \mathbb{R}^{N \times d_u}$, where d_u represents the encoding dimension, we combine it with the original node features denoted by X . This concatenation process results in a new feature matrix X^* , defined as follows: $X^* = [X, U]$. For further details on incorporating relative encodings, please refer to Appendix B.1.

3.2 Local Propagation Block (LCB)

Local Propagation Block (LCB) aggregates neighborhood embeddings for each node and concatenates them with the original ones by utilizing the explicit topological information present in the adjacency matrix. Notably, *no parameters* are involved at this stage, making it akin to the traditional feature propagation with a dense skip connection. LCB can be expressed as follows:

$$h_v^{*(l)} = [h_v^{(l-1)}, \alpha_v^{(l)}] \quad \text{or} \quad H^{*(l)} = [H^{(l-1)}, AH^{(l-1)}] \quad (4)$$

where $\alpha_v^{(l)}$ and $h_v^{(l-1)}$ are defined as before. Instead of adding self-edges for each node, we concatenate $\alpha_v^{(l)}$ and $h_v^{(l-1)}$, enabling our model to distinguish node and propagation embeddings. Moreover, rather than solely relying on $h_v^{(l)}$, local attention mechanisms similar to those found in GAT [21] can be incorporated. Alternative approaches for LCB are further discussed in Section 4.3.

Proposition 3.1. *LCB can be computed in $\mathcal{O}(N + M)$ using Sparse Matrix Matrix (SpMM) multiplication between $X^{(l)}$ and A in linear time complexity, where $M = |E|$.*

3.3 Global Context Block (GCB)

Efforts have aimed at creating efficient attention alternatives to capture longer contexts via low-rank approximation, factorization, and sparsification, often leading to trade-offs between efficiency and quality [46]. Meanwhile, recent sequence models opt for linear convolutions or RNNs which offer near-linear time complexity [41, 44, 47, 18, 19, 48]. Building upon the evolving research, for the first time, we explore whether global convolutions can capture global context within graph structures.

However, designed for sequences, many of the global convolutional models lack graph handling capabilities inherently. This leads us to a key question: Can we develop an operator that effectively processes graphs using global convolutions? Our investigation has yielded positive results, leading to Global Context Block (GCB), a novel operator with graph awareness. Below, we highlight the key distinctions and enhancements of GCB compared to Hyena. Furthermore, we provide ablation studies and empirical comparisons in Section 4.3 that demonstrate significant quality improvements.

Graph-to-sequence: Since we focus on graphs, we arrange both A and X using permutation π and convert them into time-correlated sequences, aligning node IDs with time (t).

All-to-all information flow: As our setup lacks causality unlike sequences, we remove the causal mask from the global convolution kernel. This allows information to flow mutually between all nodes, respecting the natural dynamics of graph data. The non-causal filters are vital because the relationship between nodes is not inherently sequential or unidirectional. Nodes can have mutual or bidirectional influences, and their relationships are not bound by a linear sequence like words in a sentence.

Graph-aware context: (1) The original proposal by [18] for global convolutional models for sequences involves exponential decay modulation for convolution filters, assigning higher weights to nearby points in the sequence. In contrast, we aim to minimize the impact of the permutation π during model training. Therefore, we treat all nodes equally regardless of their distance under π by eliminating this decay. (2) Unlike Hyena [19], GECO does not employ short convolution along the sequence length, as π may not reflect a locality-sensitive order. Instead, GECO utilizes LCB for local dependencies by leveraging the adjacency matrix. In addition, we first apply LCB before generating input projections, which further reduces the number of parameters in comparison to the prior work.

Window of the global convolution: We set the window size for global convolutions to match the number of nodes, ensuring the inclusion of all nodes within the convolution operation. Without the adjacency matrix, no explicit context is present for graphs. Thus, shorter window lengths hold no meaningful interpretation. This is similarly reasoned by the natural dynamics of graph data where node permutations do not introduce proximity-based context.

Algorithm 1 presents the GCB (notations unified with [19]). Given a node embedding matrix X , GCB generates $(K + 1)$ projections, where K is a hyperparameter controlling its recurrence. In this work, we set $K = 2$, and in this case, the three projections serve roles similar to query, key, and value. For each projection, a filter is learned by a simple FFN, with node IDs used for filters’ positional encoding. Subsequently, the value V is updated using global convolutions with one projection and filter at a time, followed by element-wise multiplication gating, until all projections are processed. GCB is formally expressed as:

Algorithm 1 Forward pass of GCB Operator

Input: Node embeddings $\mathbf{X} \in \mathbb{R}^{N \times d}$; Order K ; PE dim d_e ;
 1. $P_1, \dots, P_K, V = \text{Projection}(\mathbf{X})$ # Linear projections P_i
 2. $F_1, \dots, F_K = \text{Filter}(N, d_e)$ # Position based filters F_i
 # Update V until all projections are exhausted
for $i = 1, \dots, K$ **do**
 3. In parallel across d : $V_i \leftarrow (P_i)_t \cdot \text{FFTConv}(F_i, V)_t$
end for
 4. Return V

$$y = v \odot (f_q * (q \odot (f_k * k))) \tag{5}$$

We assume single-channel features and omit layer notations for simplicity. $q, k, v \in \mathbb{R}^{N \times 1}$ are linear projections of the input, and $f_k, f_q \in \mathbb{R}^{N \times 1}$ are learnable filters with circular symmetry. \odot denotes Hadamard product (element-wise multiplication), and $*$ denotes circular convolution.

3.4 Surrogate Attention Analysis

One natural question that arises is why the GCB is a meaningful replacement for GT’s self-attention. To answer this, we can rewrite the attention matrix as $\text{Attn}(H) = \text{Softmax}\left(\frac{HW_Q(HW_K)^T}{\sqrt{d}}\right)$ and

interpret it as a normalized adjacency matrix, where the pairwise similarity scores are edge weights learned through the attention mechanism. GCB with its modified filter design also learns a surrogate attention matrix that can be interpreted as an adjacency matrix that takes the global context into account. However, it is computed efficiently without storing the entire dense matrix. Consequently, this design allows us to scale to larger datasets using the same computing resources. Please refer to Appendix D.1 for details on the surrogate attention matrix decomposition.

Proposition 3.2. *GCB computes a surrogate attention matrix in $\mathcal{O}(N \log N)$ by using Fast Fourier Transform (FFT) and element-wise multiplication.*

3.5 Pitfalls of Permutation Sensitivity and Mitigation Strategies

The GECO has certain pitfalls in terms of permutation sensitivity. While typical GNNs use permutation invariant functions [3, 20], GCB’s short and global convolutions are shift-invariant but not permutation invariant. Importantly, a line of research focuses on order-sensitive GNNs [49, 50, 51, 52, 53, 54] for enhanced expressibility. Notably GraphSAGE [20] and [55] with LSTM have shown outperforming results. However, while these models may improve quality for a specific task, the model could potentially lose its generalizability. By replacing short convolutions with LCB, we make the local mixing permutation invariant. However, global convolutions remain order-sensitive. To mitigate GCB’s permutation sensitivity, we have explored different random permutation strategies.

Static Random: We randomly permute the graph once before training as a naive baseline and compare the performance variations between different runs. Surprisingly, we observed that the final results are not significantly impacted by different orderings, which we elaborate in Section 4.3.

Dynamic Random: With $N!$ permutations sampled, a permutation-sensitive function can recover a permutation-invariant function [49]. Formally, consider parametrized function \vec{f} with parameters W , and permutation π . The original target permutation invariant function $\bar{\vec{f}}$ can be recovered as:

$$\bar{\vec{f}}(X; W) = \frac{1}{N!} \sum_{\pi \in \Pi_N} \vec{f}(A_\pi, X_\pi; W) \quad (6)$$

However, $N!$ is intractable for large graphs, so one option is to sample permutations during training. Consequently, we sample a random permutation per epoch per layer during model training. Similar strategies have been also used for positional encodings, such as random sign flipping for Laplacian PE [16]. This helps model to see many different permutations during training, potentially memorize permutation invariance and gain robustness to different permutations. π -SGD [49] theoretically proved such strategies approximates $\bar{\vec{f}}$ with decreasing variance as more permutations are sampled.

Proposition 3.3. *GECO with dynamic random sampling strategy is an approximate solution to original target permutation invariant function.*

For detailed proof, refer to Appendix D.2. While we observe robustness to different orderings, understanding and addressing this limitation is crucial for broadening the applicability of GECO.

3.6 End-to-End Training

Algorithm 2 presents the end-to-end training with dynamic permutation. We start by positional encodings. The training is further broken into two main blocks. LCB propagates neighborhood embeddings and applies normalization, which is followed by GCB. Each GECO is followed by an FFN, such that $\text{FFN}(X) = \sigma(XW_1)W_2$, where $W_1, W_2 \in \mathbb{R}^{d \times d}$ are the linear layer weights. Both the GECO and FFN use skip connections, normalization, and dropout. Alternatively, line 2 can be moved out of

Algorithm 2 End-to-end GECO Model Training

Input: Adj. matrix $\mathbf{A} \in \mathbb{R}^{N \times N}$; Node features $\mathbf{X} \in \mathbb{R}^{N \times d}$; Edge features $\mathcal{E} \in \mathbb{R}^{M \times d_e}$;

1. $\mathbf{X}, \mathbf{A} = \text{GraphPositionalEncoder}(\mathbf{X}, \mathbf{A}, \mathcal{E})$
 - for** $\ell = 0, \dots, L - 1$ **do**
 2. $\pi = \text{SamplePermutation}()$
 3. $\mathbf{X}^{(0)} = \text{Permute}(\mathbf{A}, \mathbf{X}, \pi)$
 4. $\mathbf{X}^{(l+1)} = \text{LayerNorm}(\text{GECO}(\mathbf{X}^{(l)}, \mathbf{A}) + \mathbf{X}^{(l)})$
 5. $\mathbf{X}^{(l+1)} = \text{LayerNorm}(\text{FFN}(\mathbf{X}^{(l+1)}) + \mathbf{X}^{(l+1)})$
 - end for**
 5. Return $\mathbf{X}^L \in \mathbb{R}^{N \times D}$
-

the for loop to achieve static permutation strategy to order the nodes as a preprocessing step. GECO uses three quasilinear operators and can be computed in $\mathcal{O}(N \log N + M)$. For the complete algorithm and complexity analysis, refer to Appendices B.2 and E.2 respectively.

3.7 Comparison with Prior Work

Hybrid Approaches. Prior works [12, 10, 56, 57] straightforwardly combine off-the-shelf GNNs and Transformers as separate local and global modules. In contrast, GECO’s LCB and GCB are not auxiliary modules but integrated components of a new compact layer design, refining the model by removing intermediate parameters and non-linearities. This design uses skip connections for the entire layer rather than separate components. Please refer to Appendices G.4 and G.6 for details.

NAgphormer’s Hop2Token is a preprocessing step decoupled from model training, where feature propagation iterations are performed to generate node tokens [23]. Such decoupling methods separate training from feature propagation, hindering model to learn complex relationships between consecutive layers [58]. In contrast, LCB’s feature propagation is coupled with learnable parameters of GCB. LCB is not a preprocessing step but rather an integral pre-step to GCB during model training. In Appendix G.7, we further discuss NAgphormer’s recovery as a specific JKNets [59] instance.

Graph-Mamba [60] has recently adapted Mamba [61] for graphs. It focuses on node ordering strategies based on prioritization while using off-the-shelf permutation-sensitive components. In contrast, we refine the layer design, introduce LCB, aim to mitigate permutation-sensitivity, and further incorporate random permutation strategies for improved robustness. Notably, our evaluation also targets large node prediction datasets, unlike Graph-Mamba’s focus on small graph-level tasks.

Orthogonal research: (1) *Model-agnostic methods:* Universally applicable feature encoding and initialization/tuning methods [10, 25, 11, 62, 26, 27, 63, 28]. (2) *Scaling methods* such as GOAT [37], HSGT [36], and LargeGT [64] that leverage self-attention. GECO offers an alternative kernel combinable with these methods. Section 4.3 provides evidence on when this combination is beneficial based on input size. While Graph-ViT/MLP-Mixer propose alternatives, they are limited to graph-level tasks and require graph re-partitioning at every epoch, which can be costly for large node-level tasks. In contrast, GECO does not require partitioning and is applicable to node-level tasks as well.

4 Experiments

Table 1: LRGB Eval.: the **first**, **second**, and **third** are highlighted. We reuse the results from [29, 31].

Model	PascalVOC-SP	COCO-SP	Peptides-func	Peptides-struct	PCQM-Contact
	F1 score \uparrow	F1 score \uparrow	AP \uparrow	MAE \downarrow	MRR \uparrow
GCN	0.1268 \pm 0.0060	0.0841 \pm 0.0010	0.5930 \pm 0.0023	0.3496 \pm 0.0013	0.3234 \pm 0.0006
GINE	0.1265 \pm 0.0076	0.1339 \pm 0.0044	0.5498 \pm 0.0079	0.3547 \pm 0.0045	0.3180 \pm 0.0027
GatedGCN	0.2873 \pm 0.0219	0.2641 \pm 0.0045	0.5864 \pm 0.0077	0.3420 \pm 0.0013	0.3218 \pm 0.0011
GatedGCN+RWSE	0.2860 \pm 0.0085	0.2574 \pm 0.0034	0.6069 \pm 0.0035	0.3357 \pm 0.0006	0.3242 \pm 0.0008
Transformer+LapPE	0.2694 \pm 0.0098	0.2618 \pm 0.0031	0.6326 \pm 0.0126	0.2529 \pm 0.0016	0.3174 \pm 0.0020
SAN+LapPE	0.3230 \pm 0.0039	0.2592 \pm 0.0158	0.6384 \pm 0.0121	0.2683 \pm 0.0043	0.3350 \pm 0.0003
SAN+RWSE	0.3216 \pm 0.0027	0.2434 \pm 0.0156	0.6439 \pm 0.0075	0.2545 \pm 0.0012	0.3341 \pm 0.0006
GPS w/ Transformer	0.3748 \pm 0.0109	0.3412 \pm 0.0044	0.6535 \pm 0.0041	0.2500 \pm 0.0005	0.3337 \pm 0.0006
Exphormer	0.3975 \pm 0.0037	0.3455 \pm 0.0009	0.6527 \pm 0.0043	0.2481 \pm 0.0007	0.3637 \pm 0.0020
GECO (Ours)	0.4210 \pm 0.0080	0.3320 \pm 0.0032	0.6975 \pm 0.0025	0.2464 \pm 0.0009	0.3526 \pm 0.0016

4.1 Objective 1: Prediction Quality

We assess the GECO on ten benchmarks outlined in Appendix A.1, where each dataset contains many small graphs, with an average number of nodes ranging from tens to five hundred. Consequently, **scalability is not a significant concern** for these datasets as the computational load is determined by the average number of nodes. As evidence, even the most computation-intensive GTs, such as Graphormer or GraphGPS with MHA, can be trained on these datasets using Nvidia-V100 (32GB) or Nvidia-A100 (40GB) GPUs [11, 29]. The experiments in this section aim to demonstrate GECO’s competitive predictive quality compared to GT baselines, as many of them encounter memory or time issues with larger graphs. Nevertheless, for these evaluations, we begin by creating a hybrid GNN+GECO by replacing the attention module used in GraphGPS. For dataset and hyperparameter details please refer to Appendix A and Appendix F.3, respectively.

Long Range Graph Benchmark (LRGB). Table 1 presents our evaluation on the LRGB, a collection of graph tasks designed to test a model’s ability to capture long-range dependencies. The results show that GECO outperforms baselines across most datasets, with improvements up-to 4.3%. For

the remaining datasets, it ranks among the top three, with quality within 1.3% of the best baseline. By capturing long-range dependencies effectively, GECO surpasses the performance of MHA in most cases without compromising quality. Notably, GECO’s F1 score on PascalVOC increased from 0.4053 to 0.4210 without positional encodings, resulting in enhanced quality with a simplified model.

Table 2: OGBG Eval.: **the best** is highlighted. We reuse the results from [29].

Model	ogbg-molhiv	ogbg-molpcba	ogbg-ppa	ogbg-code2
	AUROC \uparrow	Avg. Precision \uparrow	Accuracy \uparrow	F1 score \uparrow
SAN	0.7785 \pm 0.2470	0.2765 \pm 0.0042	–	–
GraphTrans (GCN-Virtual)	–	0.2761 \pm 0.0029	–	0.1830 \pm 0.0024
K-Subtree SAT	–	–	0.7522 \pm 0.0056	0.1937 \pm 0.0028
GPS	0.7880 \pm 0.0101	0.2907 \pm 0.0028	0.8015 \pm 0.0033	0.1894 \pm 0.0024
GECO	0.7980 \pm 0.0200	0.2961 \pm 0.0008	0.7982 \pm 0.0042	0.1915 \pm 0.002

Open Graph Benchmark (OGB). Table 2 presents the evaluation results on OGB Graph level tasks. For clarity, we only compare GT methods, but full table can be found in Appendix G.3. Similar to GraphGPS, we observed instances of overfitting. Nevertheless, GECO outperforms GraphGPS on the majority of the datasets, except for ppa. Across all datasets, it consistently secures the top two, demonstrating its effectiveness as a high-quality and efficient GT alternative.

Table 3: PCQM4Mv2 Eval.: the **first**, **second**, and **third** are highlighted. *Validation* set is used for evaluation as *test* set is private. We reuse results from [29].

PCQM4Mv2	GCN	GCN-virtual	GIN-virtual	GRPE	EGT	Graphormer	GPS-sm	GPS-med	GECO
Train MAE \downarrow	n/a	n/a	n/a	n/a	n/a	0.0348	0.0653	0.0726	0.0578
Val. MAE \downarrow	0.1379	0.1153	0.1083	0.0890	0.0869	0.0864	0.0938	0.0858	0.0841
# Param.	2.0M	4.9M	6.7M	46.2M	89.3M	48.3M	6.2M	19.4M	6.2M

PCQM4Mv2. Table 3 demonstrates that GECO outperforms both GNN and GT baselines on PCQM4Mv2 in terms of prediction quality. Notably, GECO uses only **1/8** and **1/3** of the parameters required by Graphormer and GraphGPS, respectively. This parameter reduction brings GECO in close proximity to the parameter count used by GNN baselines, while boosting their quality.

4.2 Objective 2: Scalability for Larger Graphs

Table 4: Accuracy on large node prediction datasets: the **first**, **second**, and **third** are highlighted. We reuse the results from [65, 31, 66], and run Exphormer locally except Arxiv. – indicates that the data was either not included in the original work or could not be successfully reproduced.

Model	Flickr	Arxiv	Reddit	Yelp
	Accuracy	Accuracy	Accuracy	Micro-F1 Score
GCN	50.90 \pm 0.12	70.25 \pm 0.22	92.78 \pm 0.11	40.08 \pm 0.15
SAGE	53.72 \pm 0.16	72.00 \pm 0.16	96.50 \pm 0.03	63.03 \pm 0.20
GraphSaint	51.37 \pm 0.21	67.95 \pm 0.24	95.58 \pm 0.07	29.42 \pm 1.32
Cluster-GCN	49.95 \pm 0.15	68.00 \pm 0.59	95.70 \pm 0.06	56.39 \pm 0.64
GAT	50.70 \pm 0.32	71.59 \pm 0.38	96.50 \pm 0.11	61.58 \pm 1.37
Graphormer	OOM	OOM	OOM	OOM
Graphormer-SAMPLE	51.93 \pm 0.21	70.43 \pm 0.20	93.05 \pm 0.22	60.01 \pm 0.45
SAN	OOM	OOM	OOM	OOM
SAT	OOM	OOM	OOM	OOM
SAT-SAMPLE	50.48 \pm 0.34	68.20 \pm 0.46	93.37 \pm 0.32	60.32 \pm 0.65
ANS-GT	–	68.20 \pm 0.46	95.30 \pm 0.81	–
GraphGPS w/ Transformer	OOM	OOM	OOM	OOM
Exphormer	52.60 \pm 0.18	72.44 \pm 0.28	95.90 \pm 0.15	60.80 \pm 1.56
HSGT	54.12 \pm 0.51	72.58 \pm 0.31	–	63.47 \pm 0.45
GECO (Ours)	55.55 \pm 0.25	73.10 \pm 0.24	96.65 \pm 0.05	63.18 \pm 0.59

We assess GECO on 4 benchmark datasets where each graph contains a much larger number of nodes. Notably, traditional Dense GTs struggle to handle such large graphs due to their quadratic complexity while GECO succeeds with its superior computational and memory efficiency. In the following experiments, we design our models using only GECO blocks, following Algorithm 2. For

simplicity, we avoid using structural/positional encodings as computing them may be infeasible for large graphs. For details on datasets and hyperparameters, please refer to Appendices A.2 and F.3.

Unlike previous works that exhibit a trade-off between quality and scalability, GECO scales efficiently to large datasets and achieves superior quality across all compared to Dense GTs (Graphormer/GraphGPS), which suffer from OOM/timeout issues. Remarkably, GECO demonstrates significant predictive superiority, surpassing Dense GT baseline methods by up to 4.5%. On Arxiv, GECO outperforms recently proposed GT works Exphormer and GOAT [37] up to 0.7%. Notably, Graphormer with sampling falls short in achieving competitive quality across all datasets. When comparing GECO to various baselines, including orthogonal methods, GECO remains competitive. It outperforms various baselines on Flickr, Arxiv, and Reddit, except for Yelp where the coarsening approach HSGT [36] surpasses GECO. We leave the exploration of combining GECO with orthogonal methods such as expander graphs [31], hierarchical learning [36], and dimensionality reduction [37] as future work to potentially get even better results. Overall, the results highlight that the global context can enhance the modeling quality for large node prediction datasets, justifying our motivation to find efficient high-quality attention alternatives. To the best of our knowledge, GECO is the first attempt to capture pairwise node relations without heuristics at scale. Our evaluation illustrates its effectiveness as a Dense GT alternative for large graphs.

Table 5: Accuracy across large datasets with different permutation strategies (Natural/Static Random/Dynamic Random) with GECO, alongside a comparison with default Hyena [19].

Dataset	Hyena	GECO	GECO	GECO
Permutation	Natural	Natural	Static Random	Dynamic Random
Flickr	46.97 ± 0.08	55.55 ± 0.25	55.73 ± 0.27	55.80 ± 0.38
Arxiv	56.04 ± 0.61	73.10 ± 0.24	73.08 ± 0.28	73.12 ± 0.22
Reddit	69.24 ± 0.54	96.65 ± 0.05	96.62 ± 0.05	96.68 ± 0.06
Yelp	50.08 ± 0.31	63.18 ± 0.59	63.23 ± 0.50	63.20 ± 0.42

4.3 Ablation Studies

Permutation Robustness. In Table 5, we investigate GECO’s robustness to different permutations. First, we maintained the natural ordering of the graph and reported the mean and std of 10 runs with distinct seeds on this fixed permutation (Natural). Then, we repeated the same process, but we have applied static and dynamic permutation strategies detailed in Section 3.5. The results indicate negligible differences between different strategies with dynamic random showing slightly higher mean on multiple datasets. However, all strategies seems to fall into similar confidence intervals, hence we favor the simpler strategy in our experiments.

Hyena Comparison. Table 5 compares GECO with the off-the-shelf Hyena by setting its filter size as the entire graph. GECO consistently outperforms the off-the-shelf Hyena with a significant margin. This underscores the effectiveness of GECO, particularly in its application of global convolutions for graph structures, and distinctly sets it apart from the off-the-shelf Hyena.

Local Propagation Block Alternatives. In GECO, we adopted LCB for graph-aware local context modeling instead of using 1D convolutions originally used in Hyena. This is motivated by the limitation of 1D convolutions in capturing local dependencies in graphs where node order does not imply proximity. At Table 6, we focus on exploring alternatives to LCB within our GECO module. We experimented with replacing LCB with 1D convolutions of various filter sizes to help understand its effectiveness. We consistently

Table 6: Ablation study on the LCB alternatives: the **first**, **second**, and **third** are highlighted. Conv- x indicates 1D Convolution with a filter size of x .

Model	Local Block	Pas.VOC-SP	Pep.-func	Pep.-struct
		F1 ↑	AP ↑	MAE ↓
Transformer	N/A	0.2762	0.6333	0.2525
Performer	N/A	0.2690	0.5881	0.2739
GECO	Conv-1	0.2752	0.6589	0.2587
GECO	Conv-10	0.1757	0.6819	0.2516
GECO	Conv-20	0.1645	0.6706	0.2534
GECO	Conv-40	0.1445	0.6517	0.2547
GECO	LCB	0.3220	0.6876	0.2454

observed a diminishing trend in quality as filter sizes increased, which can be attributed to larger filter sizes leading to a mix of unrelated nodes within the graph. In contrast, GECO with LCB consistently outperformed its alternatives as well as the Transformer and Performer, highlighting its effectiveness in capturing local graph dependencies.

Scaling Study. Figure 2 shows GECO’s speedup w.r.t. the optimized attention, FlashAttention [67], for increasing numbers of nodes using synthetic datasets with similar sparsity patterns to those in Table 4. The results highlight that the speedup linearly increases with the number of nodes, and GECO reaches $169\times$ speedup on a graph with 2M nodes, confirming its relative scalability. Details including runtime numbers can be found in Appendix G.1.

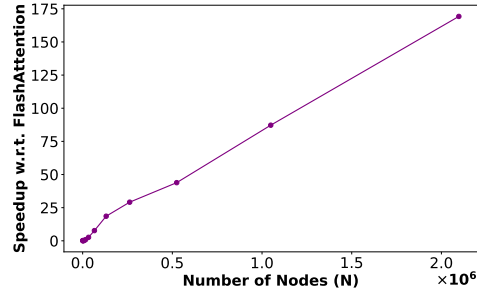


Figure 2: Relative speedup of GECO w.r.t. FlashAttention [67] characterized by $\mathcal{O}(N/\log N)$

5 Conclusion

We presented GECO, a novel graph learning model that replaces the compute-intensive MHA in GTs with an efficient and high-quality operator. With comprehensive evaluation, we demonstrated GECO effectively scales to large datasets without compromising quality, and even outperforms it. Moving forward, we plan to explore alternatives for GCB, and combinations with orthogonal approaches such as hierarchical learning.

Acknowledgement

This work was partially done when the first author was a research scientist intern at Meta AI. This work was partially supported by the NSF grant CCF-1919021.

References

- [1] M. Gori, G. Monfardini, and F. Scarselli. A new model for learning in graph domains. In *Proceedings. 2005 IEEE International Joint Conference on Neural Networks, 2005.*, volume 2, pages 729–734 vol. 2, 2005.
- [2] Franco Scarselli, Marco Gori, Ah Chung Tsoi, Markus Hagenbuchner, and Gabriele Monfardini. The graph neural network model. *IEEE Transactions on Neural Networks*, 20(1):61–80, 2009.
- [3] Thomas N. Kipf and Max Welling. Semi-supervised classification with graph convolutional networks. In *International Conference on Learning Representations*, 2017.
- [4] Muhan Zhang and Yixin Chen. Link prediction based on graph neural networks. *Advances in neural information processing systems*, 31, 2018.
- [5] Muhan Zhang, Zhicheng Cui, Marion Neumann, and Yixin Chen. An end-to-end deep learning architecture for graph classification. In *Proceedings of the AAAI conference on artificial intelligence*, volume 32, 2018.
- [6] Vijay Prakash Dwivedi, Ladislav Rampásek, Michael Galkin, Ali Parviz, Guy Wolf, Anh Tuan Luu, and Dominique Beaini. Long range graph benchmark. *Advances in Neural Information Processing Systems*, 35:22326–22340, 2022.
- [7] Qimai Li, Zhichao Han, and Xiao-Ming Wu. Deeper insights into graph convolutional networks for semi-supervised learning. In *Thirty-Second AAAI conference on artificial intelligence*, 2018.
- [8] Uri Alon and Eran Yahav. On the bottleneck of graph neural networks and its practical implications. In *International Conference on Learning Representations*, 2020.
- [9] Jake Topping, Francesco Di Giovanni, Benjamin Paul Chamberlain, Xiaowen Dong, and Michael M. Bronstein. Understanding over-squashing and bottlenecks on graphs via curvature. In *International Conference on Learning Representations*, 2022.
- [10] Vijay Prakash Dwivedi and Xavier Bresson. A generalization of transformer networks to graphs. *arXiv preprint arXiv:2012.09699*, 2020.

- [11] Chengxuan Ying, Tianle Cai, Shengjie Luo, Shuxin Zheng, Guolin Ke, Di He, Yanming Shen, and Tie-Yan Liu. Do transformers really perform badly for graph representation? In A. Beygelzimer, Y. Dauphin, P. Liang, and J. Wortman Vaughan, editors, *Advances in Neural Information Processing Systems*, 2021.
- [12] Zhanghao Wu, Paras Jain, Matthew Wright, Azalia Mirhoseini, Joseph E Gonzalez, and Ion Stoica. Representing long-range context for graph neural networks with global attention. *Advances in Neural Information Processing Systems*, 34:13266–13279, 2021.
- [13] Ashish Vaswani, Noam Shazeer, Niki Parmar, Jakob Uszkoreit, Llion Jones, Aidan N Gomez, Łukasz Kaiser, and Illia Polosukhin. Attention is all you need. *Advances in neural information processing systems*, 30, 2017.
- [14] Scott Freitas, Yuxiao Dong, Joshua Neil, and Duen Horng Chau. A large-scale database for graph representation learning. In *Thirty-fifth Conference on Neural Information Processing Systems Datasets and Benchmarks Track (Round 1)*, 2021.
- [15] Weihua Hu, Matthias Fey, Hongyu Ren, Maho Nakata, Yuxiao Dong, and Jure Leskovec. Ogb-lsc: A large-scale challenge for machine learning on graphs. In *Thirty-fifth Conference on Neural Information Processing Systems Datasets and Benchmarks Track (Round 2)*, 2021.
- [16] Vijay Prakash Dwivedi, Chaitanya K Joshi, Anh Tuan Luu, Thomas Laurent, Yoshua Bengio, and Xavier Bresson. Benchmarking graph neural networks. *Journal of Machine Learning Research*, 24(43):1–48, 2023.
- [17] David W. Romero, Anna Kuzina, Erik J Bekkers, Jakub Mikolaj Tomczak, and Mark Hoogendoorn. CKConv: Continuous kernel convolution for sequential data. In *International Conference on Learning Representations*, 2022.
- [18] Yuhong Li, Tianle Cai, Yi Zhang, Deming Chen, and Debadeepta Dey. What makes convolutional models great on long sequence modeling? In *The Eleventh International Conference on Learning Representations*, 2023.
- [19] Michael Poli, Stefano Massaroli, Eric Nguyen, Daniel Y Fu, Tri Dao, Stephen Baccus, Yoshua Bengio, Stefano Ermon, and Christopher Ré. Hyena hierarchy: Towards larger convolutional language models. In *International Conference on Machine Learning*, 2023.
- [20] Will Hamilton, Zhitao Ying, and Jure Leskovec. Inductive representation learning on large graphs. *Advances in neural information processing systems*, 30, 2017.
- [21] Petar Veličković, Guillem Cucurull, Arantxa Casanova, Adriana Romero, Pietro Liò, and Yoshua Bengio. Graph attention networks. In *International Conference on Learning Representations*, 2018.
- [22] Keyulu Xu, Weihua Hu, Jure Leskovec, and Stefanie Jegelka. How powerful are graph neural networks? In *International Conference on Learning Representations*, 2019.
- [23] Jinsong Chen, Kaiyuan Gao, Gaichao Li, and Kun He. NAGphormer: A tokenized graph transformer for node classification in large graphs. In *The Eleventh International Conference on Learning Representations*, 2023.
- [24] Dongqi Fu, Zhigang Hua, Yan Xie, Jin Fang, Si Zhang, Kaan Sancak, Hao Wu, Andrey Malevich, Jingrui He, and Bo Long. VCR-graphormer: A mini-batch graph transformer via virtual connections. In *The Twelfth International Conference on Learning Representations*, 2024.
- [25] Devin Kreuzer, Dominique Beaini, William L. Hamilton, Vincent Létourneau, and Prudencio Tossou. Rethinking graph transformers with spectral attention. In A. Beygelzimer, Y. Dauphin, P. Liang, and J. Wortman Vaughan, editors, *Advances in Neural Information Processing Systems*, 2021.
- [26] Dexiong Chen, Leslie O’Bray, and Karsten Borgwardt. Structure-aware transformer for graph representation learning. In *International Conference on Machine Learning*, pages 3469–3489. PMLR, 2022.

- [27] Haiteng Zhao, Shuming Ma, Dongdong Zhang, Zhi-Hong Deng, and Furu Wei. Are more layers beneficial to graph transformers? In *The Eleventh International Conference on Learning Representations*, 2023.
- [28] Liheng Ma, Chen Lin, Derek Lim, Adriana Romero-Soriano, Puneet K Dokania, Mark Coates, Philip Torr, and Ser-Nam Lim. Graph inductive biases in transformers without message passing. In *International Conference on Machine Learning*, pages 23321–23337. PMLR, 2023.
- [29] Ladislav Rampasek, Mikhail Galkin, Vijay Prakash Dwivedi, Anh Tuan Luu, Guy Wolf, and Dominique Beaini. Recipe for a general, powerful, scalable graph transformer. In Alice H. Oh, Alekh Agarwal, Danielle Belgrave, and Kyunghyun Cho, editors, *Advances in Neural Information Processing Systems*, 2022.
- [30] Manzil Zaheer, Guru Guruganesh, Kumar Avinava Dubey, Joshua Ainslie, Chris Alberti, Santiago Ontanon, Philip Pham, Anirudh Ravula, Qifan Wang, Li Yang, et al. Big bird: Transformers for longer sequences. *Advances in neural information processing systems*, 33:17283–17297, 2020.
- [31] Hamed Shirzad, Ameya Velingker, Balaji Venkatachalam, Danica J Sutherland, and Ali Kemal Sinop. Exphormer: Sparse transformers for graphs. In *International Conference on Machine Learning*, 2023.
- [32] Xiaoxin He, Bryan Hooi, Thomas Laurent, Adam Perold, Yann LeCun, and Xavier Bresson. A generalization of vit/mlp-mixer to graphs. In *International Conference on Machine Learning*, pages 12724–12745. PMLR, 2023.
- [33] Alexey Dosovitskiy, Lucas Beyer, Alexander Kolesnikov, Dirk Weissenborn, Xiaohua Zhai, Thomas Unterthiner, Mostafa Dehghani, Matthias Minderer, Georg Heigold, Sylvain Gelly, et al. An image is worth 16x16 words: Transformers for image recognition at scale. *arXiv preprint arXiv:2010.11929*, 2020.
- [34] Ilya O Tolstikhin, Neil Houlsby, Alexander Kolesnikov, Lucas Beyer, Xiaohua Zhai, Thomas Unterthiner, Jessica Yung, Andreas Steiner, Daniel Keysers, Jakob Uszkoreit, et al. Mlp-mixer: An all-mlp architecture for vision. *Advances in neural information processing systems*, 34:24261–24272, 2021.
- [35] Zaxixi Zhang, Qi Liu, Qingyong Hu, and Chee-Kong Lee. Hierarchical graph transformer with adaptive node sampling. In Alice H. Oh, Alekh Agarwal, Danielle Belgrave, and Kyunghyun Cho, editors, *Advances in Neural Information Processing Systems*, 2022.
- [36] Wenhao Zhu, Tianyu Wen, Guojie Song, Xiaojun Ma, and Liang Wang. Hierarchical transformer for scalable graph learning. *arXiv preprint arXiv:2305.02866*, 2023.
- [37] Kezhi Kong, Jiu-hai Chen, John Kirchenbauer, Renkun Ni, C. Bayan Bruss, and Tom Goldstein. GOAT: A global transformer on large-scale graphs. In *Proceedings of the 40th International Conference on Machine Learning*. PMLR, 2023.
- [38] Cameron Diao and Ricky Loynd. Relational attention: Generalizing transformers for graph-structured tasks. In *The Eleventh International Conference on Learning Representations*, 2023.
- [39] Yann LeCun, Léon Bottou, Yoshua Bengio, and Patrick Haffner. Gradient-based learning applied to document recognition. *Proceedings of the IEEE*, 1998.
- [40] Yi Tay, Mostafa Dehghani, Samira Abnar, Yikang Shen, Dara Bahri, Philip Pham, Jinfeng Rao, Liu Yang, Sebastian Ruder, and Donald Metzler. Long range arena : A benchmark for efficient transformers. In *International Conference on Learning Representations*, 2021.
- [41] Albert Gu, Karan Goel, and Christopher Re. Efficiently modeling long sequences with structured state spaces. In *International Conference on Learning Representations*, 2021.
- [42] Jimmy T.H. Smith, Andrew Warrington, and Scott Linderman. Simplified state space layers for sequence modeling. In *International Conference on Learning Representations*, 2023.

- [43] Daniel Y Fu, Elliot L Epstein, Eric Nguyen, Armin W Thomas, Michael Zhang, Tri Dao, Atri Rudra, and Christopher Re. Simple hardware-efficient long convolutions for sequence modeling. In *ICLR 2023 Workshop on Mathematical and Empirical Understanding of Foundation Models*, 2023.
- [44] Daniel Y Fu, Tri Dao, Khaled Kamal Saab, Armin W Thomas, Atri Rudra, and Christopher Re. Hungry hungry hippos: Towards language modeling with state space models. In *International Conference on Learning Representations*, 2023.
- [45] Vijay Prakash Dwivedi, Anh Tuan Luu, Thomas Laurent, Yoshua Bengio, and Xavier Bresson. Graph neural networks with learnable structural and positional representations. In *International Conference on Learning Representations*, 2022.
- [46] Fabio Catania, Micol Spitale, and Franca Garzotto. Conversational agents in therapeutic interventions for neurodevelopmental disorders: A survey. *ACM Comput. Surv.*, 2023.
- [47] Bo Peng, Eric Alcaide, Quentin Anthony, Alon Albalak, Samuel Arcadinho, Huanqi Cao, Xin Cheng, Michael Chung, Matteo Grella, Kranthi Kiran GV, et al. Rwkv: Reinventing rnns for the transformer era. *arXiv preprint arXiv:2305.13048*, 2023.
- [48] Eric Nguyen, Michael Poli, Marjan Faizi, Armin Thomas, Callum Birch-Sykes, Michael Wornow, Aman Patel, Clayton Rabideau, Stefano Massaroli, Yoshua Bengio, et al. Hye-nadna: Long-range genomic sequence modeling at single nucleotide resolution. *arXiv preprint arXiv:2306.15794*, 2023.
- [49] Ryan L. Murphy, Balasubramaniam Srinivasan, Vinayak Rao, and Bruno Ribeiro. Janosy pooling: Learning deep permutation-invariant functions for variable-size inputs. In *International Conference on Learning Representations*, 2019.
- [50] Ryan Murphy, Balasubramaniam Srinivasan, Vinayak Rao, and Bruno Ribeiro. Relational pooling for graph representations. In *International Conference on Machine Learning*, pages 4663–4673. PMLR, 2019.
- [51] Zhengdao Chen, Lei Chen, Soledad Villar, and Joan Bruna. Can graph neural networks count substructures? *Advances in neural information processing systems*, 2020.
- [52] Ryoma Sato, Makoto Yamada, and Hisashi Kashima. Random features strengthen graph neural networks. In *Proceedings of the 2021 SIAM international conference on data mining (SDM)*, pages 333–341. SIAM, 2021.
- [53] Zhongyu Huang, Yingheng Wang, Chaozhuo Li, and Huiguang He. Going deeper into permutation-sensitive graph neural networks. In *International Conference on Machine Learning*, 2022.
- [54] Michail Chatzianastasis, Johannes Lutzeyer, George Dasoulas, and Michalis Vazirgiannis. Graph ordering attention networks. In *Proceedings of the AAAI Conference on Artificial Intelligence*, 2023.
- [55] John Moore and Jennifer Neville. Deep collective inference. In *Proceedings of the AAAI Conference on Artificial Intelligence*, 2017.
- [56] Kevin Lin, Lijuan Wang, and Zicheng Liu. Mesh graphormer. In *Proceedings of the IEEE/CVF international conference on computer vision*, pages 12939–12948, 2021.
- [57] Erxue Min, Runfa Chen, Yatao Bian, Tingyang Xu, Kangfei Zhao, Wenbing Huang, Peilin Zhao, Junzhou Huang, Sophia Ananiadou, and Yu Rong. Transformer for graphs: An overview from architecture perspective. *arXiv preprint arXiv:2202.08455*, 2022.
- [58] Felix Wu, Amauri Souza, Tianyi Zhang, Christopher Fifty, Tao Yu, and Kilian Weinberger. Simplifying graph convolutional networks. In *International conference on machine learning*, pages 6861–6871. PMLR, 2019.
- [59] Keyulu Xu, Chengtao Li, Yonglong Tian, Tomohiro Sonobe, Ken-ichi Kawarabayashi, and Stefanie Jegelka. Representation learning on graphs with jumping knowledge networks. In *International conference on machine learning*, pages 5453–5462. PMLR, 2018.

- [60] Chloe Wang, Oleksii Tsepa, Jun Ma, and Bo Wang. Graph-mamba: Towards long-range graph sequence modeling with selective state spaces. *arXiv preprint arXiv:2402.00789*, 2024.
- [61] Albert Gu and Tri Dao. Mamba: Linear-time sequence modeling with selective state spaces. *arXiv preprint arXiv:2312.00752*, 2023.
- [62] Grégoire Mialon, Dexiong Chen, Margot Selosse, and Julien Mairal. Graphit: Encoding graph structure in transformers. *arXiv preprint arXiv:2106.05667*, 2021.
- [63] Jan Tönshoff, Martin Ritzert, Eran Rosenbluth, and Martin Grohe. Where did the gap go? reassessing the long-range graph benchmark. In *The Second Learning on Graphs Conference*, 2023.
- [64] Vijay Prakash Dwivedi, Yozen Liu, Anh Tuan Luu, Xavier Bresson, Neil Shah, and Tong Zhao. Graph transformers for large graphs. *arXiv preprint arXiv:2312.11109*, 2023.
- [65] Xiaotian Han, Tong Zhao, Yozen Liu, Xia Hu, and Neil Shah. MLPInit: Embarrassingly simple GNN training acceleration with MLP initialization. In *The Eleventh International Conference on Learning Representations*, 2023.
- [66] Hanqing Zeng, Muhan Zhang, Yinglong Xia, Ajitesh Srivastava, Andrey Malevich, Rajgopal Kannan, Viktor Prasanna, Long Jin, and Ren Chen. Decoupling the depth and scope of graph neural networks. In *Advances in Neural Information Processing Systems*, 2021.
- [67] Tri Dao, Daniel Y. Fu, Stefano Ermon, Atri Rudra, and Christopher Ré. FlashAttention: Fast and memory-efficient exact attention with IO-awareness. In *Advances in Neural Information Processing Systems*, 2022.
- [68] Weihua Hu, Matthias Fey, Marinka Zitnik, Yuxiao Dong, Hongyu Ren, Bowen Liu, Michele Catasta, and Jure Leskovec. Open graph benchmark: Datasets for machine learning on graphs. *Advances in neural information processing systems*, 33:22118–22133, 2020.
- [69] Mark Everingham, Luc Van Gool, Christopher KI Williams, John Winn, and Andrew Zisserman. The pascal visual object classes (voc) challenge. *International journal of computer vision*, 2010.
- [70] Tsung-Yi Lin, Michael Maire, Serge Belongie, James Hays, Pietro Perona, Deva Ramanan, Piotr Dollár, and C Lawrence Zitnick. Microsoft coco: Common objects in context. In *Computer Vision—ECCV 2014: 13th European Conference, Zurich, Switzerland, September 6-12, 2014, Proceedings, Part V 13*. Springer, 2014.
- [71] Sandeep Singh, Kumardeep Chaudhary, Sandeep Kumar Dhanda, Sherry Bhalla, Salman Sadullah Usmani, Ankur Gautam, Abhishek Tuknait, Piyush Agrawal, Deepika Mathur, and Gajendra PS Raghava. Satpdb: a database of structurally annotated therapeutic peptides. *Nucleic acids research*, 2016.
- [72] Hanqing Zeng, Hongkuan Zhou, Ajitesh Srivastava, Rajgopal Kannan, and Viktor Prasanna. Graphsaint: Graph sampling based inductive learning method. In *International Conference on Learning Representations*, 2020.
- [73] Ian T Jolliffe and Jorge Cadima. Principal component analysis: a review and recent developments. *Philosophical transactions of the royal society A: Mathematical, Physical and Engineering Sciences*, 2016.
- [74] Gao Huang, Zhuang Liu, Laurens Van Der Maaten, and Kilian Q Weinberger. Densely connected convolutional networks. In *Proceedings of the IEEE conference on computer vision and pattern recognition*, pages 4700–4708, 2017.
- [75] Difan Zou, Ziniu Hu, Yewen Wang, Song Jiang, Yizhou Sun, and Quanquan Gu. Layer-dependent importance sampling for training deep and large graph convolutional networks. *Advances in neural information processing systems*, 2019.
- [76] Muhammed Fatih Balın and Ümit V. Çatalyürek. Layer-neighbor sampling — defusing neighborhood explosion in GNNs. In *Thirty-seventh Conference on Neural Information Processing Systems*, 2023.

- [77] Adam Paszke, Sam Gross, Francisco Massa, Adam Lerer, James Bradbury, Gregory Chanan, Trevor Killeen, Zeming Lin, Natalia Gimelshein, Luca Antiga, et al. Pytorch: An imperative style, high-performance deep learning library. *Advances in neural information processing systems*, 32, 2019.
- [78] Xavier Bresson and Thomas Laurent. Residual gated graph convnets. *arXiv preprint arXiv:1711.07553*, 2017.
- [79] Gabriele Corso, Luca Cavalleri, Dominique Beaini, Pietro Liò, and Petar Veličković. Principal neighbourhood aggregation for graph nets. *Advances in Neural Information Processing Systems*, 33:13260–13271, 2020.
- [80] Dominique Beaini, Saro Passaro, Vincent Létourneau, Will Hamilton, Gabriele Corso, and Pietro Liò. Directional graph networks. In *International Conference on Machine Learning*, pages 748–758. PMLR, 2021.
- [81] Jan Toenshoff, Martin Ritzert, Hinrikus Wolf, and Martin Grohe. Graph learning with 1d convolutions on random walks. *arXiv preprint arXiv:2102.08786*, 2021.
- [82] Lingxiao Zhao, Wei Jin, Leman Akoglu, and Neil Shah. From stars to subgraphs: Uplifting any GNN with local structure awareness. In *International Conference on Learning Representations*, 2022.
- [83] Md Shamim Hussain, Mohammed J Zaki, and Dharmashankar Subramanian. Global self-attention as a replacement for graph convolution. In *Proceedings of the 28th ACM SIGKDD Conference on Knowledge Discovery and Data Mining*, pages 655–665, 2022.
- [84] Wei-Lin Chiang, Xuanqing Liu, Si Si, Yang Li, Samy Bengio, and Cho-Jui Hsieh. Cluster-gcn: An efficient algorithm for training deep and large graph convolutional networks. In *Proceedings of the 25th ACM SIGKDD international conference on knowledge discovery & data mining*, pages 257–266, 2019.
- [85] Eli Chien, Jianhao Peng, Pan Li, and Olgica Milenkovic. Adaptive universal generalized pagerank graph neural network. In *International Conference on Learning Representations*, 2021.
- [86] Matthias Fey and Jan E. Lenssen. Fast graph representation learning with PyTorch Geometric. In *ICLR Workshop on Representation Learning on Graphs and Manifolds*, 2019.
- [87] Takuya Akiba, Shotaro Sano, Toshihiko Yanase, Takeru Ohta, and Masanori Koyama. Optuna: A next-generation hyperparameter optimization framework. In *Proceedings of the 25rd ACM SIGKDD International Conference on Knowledge Discovery and Data Mining*, 2019.

A Datasets

We gather a wide-ranging selection of 14 datasets, encompassing diverse graph types, tasks, and scales, collected from different sources. To facilitate understanding, we classify these datasets into two overarching groups. Each dataset in the first group comprises multiple graphs, each having small number of nodes/edges. On the other hand, the second group comprises node prediction datasets, each containing a single graph with much larger number of nodes.

A.1 Datasets with Multiple Graphs

Table 7: Statics for the Datasets with Multiple Graphs, sorted by #average nodes.

MRR: Mean Reciprocal Rank, **AP**: Average Precision, **MAE**: Mean Absolute Error.

Sparsity is calculated as $\frac{M}{N^2}$, where N and M represent the average number of nodes and edges, respectively.

Dataset	# Graphs	# Avg. Nodes	# Avg. Edges	Sparsity	Level	Task	Metric
Long Range Graph Benchmark							
PCQM-Contact	529, 434	30.1	61.0	6.79×10^{-2}	link	link ranking	MRR
Peptides-func	15, 535	150.9	307.3	1.36×10^{-2}	graph	10-task classif.	AP
Peptides-struct	15, 535	150.9	307.3	1.36×10^{-2}	graph	11-task regression	MAE
COCO-SP	123, 286	476.9	2, 693.7	1.20×10^{-2}	node	81-class classif.	F1
PascalVOC-SP	11, 355	479.4	2, 710.5	1.20×10^{-2}	node	21-class classif.	F1
Open Graph Benchmark							
PCQM4Mv2	3, 746, 620	14.1	14.6	7.25×10^{-2}	graph	regression	MAE
Molhiv	41, 127	25.5	27.5	4.29×10^{-2}	graph	binary classif.	AUROC
Molpcba	437, 929	26.0	28.1	4.13×10^{-2}	graph	128-task classif.	AP
Code2	452, 741	125.2	124.2	1.59×10^{-2}	graph	5 token sequence	F1
PPA	158, 100	243.4	2, 266.1	3.25×10^{-2}	graph	37-task classif.	Accuracy

The first group consists of datasets used by GraphGPS [29] and multiple other work in the community [32, 31]. This collection consists of datasets from 5 distinct sources, and we further divide them into 2 groups: Long Range Graph Benchmark (LRGB) [6] and Open Graph Benchmark (OGB) [68, 15]. For LRGB datasets, we respect the similar budget of 500k parameters adopted by the previous literature [6].

Splits. For these datasets, we employ the experimental setup used in GraphGPS for preprocessing and data splits, please refer to the original work for details [29].

Molhiv and Molpcba are molecular property predictions sourced from the OGB Graph (OGBG) collection [68]. These predictions are derived from MoleculeNet, and each graph in the dataset represents a molecule with atoms as nodes and chemical bonds as edges. The primary task involves making binary predictions to determine whether a molecule inhibits HIV virus replication or not.

Code2 is a dataset collection consisting of Abstract Syntax Trees (ASTs) extracted from Python definitions sourced from more than 13,000 repositories on GitHub. This dataset is also part of the OGBG. The primary objective of this task is to predict the sub-tokens that compose the method name. This prediction is based on the Python method body represented by the AST and its associated node features.

PPA is a protein association network from OGBG. It is compiled from protein-protein association networks originating from a diverse set of 1,581 species, spanning 37 distinct taxonomic groups. The primary objective of this task is to predict the taxonomic group from which a given protein association neighborhood graph originates.

PascalVOC-SP and COCO-SP are node classification datasets included in the LRGB collection. These datasets are derived from super-pixel extraction on PascalVOC [69] and MS COCO datasets [70] using the SLIC algorithm. Each super-pixel (node) in these datasets is assigned to a specific class.

PCQM4Mv2 is a molecular (quantum chemistry) dataset obtained from the OGB Large-Scale Challenge (LSC) collection, focusing on predicting the DFT (density functional theory)-calculated

HOMO-LUMO energy gap of molecules using their 2D molecular graphs—a critical quantum chemical property [15]. It is important to note that the true labels for the test-dev and test-challenge dataset splits have been kept private by the challenge organizers to avoid any bias in the evaluation process. For our evaluation, we adopted the original validation set as our test set and reserved a random sample of 150,000 molecules for the validation set, following the experimental setting employed in GraphGPS.

Peptides-func, Peptides-struct, and PCQM-Contact are molecular datasets from LRGB collection. Peptides-func and Peptides-struct are both derived from 15, 535 peptides retrieved from SATPdb [71], but they differ in their task. While Peptides-func is a graph classification task based on the peptide function, Peptides-struct is a graph regression task based on the 3D structure of the peptides. These graphs have relatively large diameters and are constructed in such a way that they necessitate long-range interaction (LRI) reasoning to achieve robust performance in their respective tasks. PCQM-Contact is derived from the PCQM4M [15], which includes available 3D structures. It has been filtered to retain only the molecules that were in contact at least once. The main objective of this dataset is to identify, at the edge level, whether two molecules have been in contact.

A.2 Datasets with Single Graph

Table 8: Overview of the graph learning dataset.

Dataset	# Nodes (N)	# Edges (M)	Sparsity ($\frac{M}{N^2}$)	# Features	# Classes
Flickr	89, 250	899, 756	1.12×10^{-4}	500	7
ogbn-arxiv	169, 343	1, 166, 243	3.97×10^{-5}	128	40
Reddit	232, 965	114, 615, 892	1.95×10^{-6}	602	41
Yelp	716, 847	13, 954, 819	2.26×10^{-6}	300	100

The second group comprises large node classification datasets, and we utilize standard accuracy metrics for evaluation, except for Yelp where we use micro-F1 following the general practice. **Splits.** For the following datasets, we use publicly available standard splits across all datasets.

Reddit⁵ [20] is a dataset derived from Reddit posts. Each node in the dataset represents a post, and two posts are connected if they have been commented on by the same user. The task is to classify which subreddit (community) a post belongs to.

Flickr and **Yelp** datasets are obtained from their respective networks [72]. In the Flickr dataset, nodes represent uploaded images, and two nodes are connected if they share common properties or attributes. In the Yelp dataset, two nodes are connected if they are considered friends within the social network.

OGBN- Arxiv is OGB Node Prediction (OGBN) dataset [68] which is a citation network that connects Computer Science papers from Arxiv. The features represent bag-of-word representations of the paper’s title and abstract. The task is to identify the area of the papers.

B Architecture Details

B.1 Relative Encodings

In Section 3.1, we discuss how to incorporate positional/structural encodings. Importantly, our algorithm does not implicitly retain a dense attention matrix, making the integration of relative encodings more challenging. We work with a relative encoding matrix $U_r \in \mathbb{R}^{N \times N}$, such as adjacency matrix or spatial information matrix, and first create a low-rank approximation [73] denoted by $U_r^* \in \mathbb{R}^{N \times d_r}$, where d_r is the rank of the approximation. Subsequently, we append the approximate relative encoding matrix to the node features and create an updated feature matrix $X^* = [X, U_r^*]$. Note that, both node and edge positional/structural encodings can be extracted offline as a preprocessing step.

⁵Reddit dataset is derived from the Pushshift.io Reddit dataset, which is a previously existing dataset extracted and obtained by a third party that contains preprocessed comments posted on the social network Reddit and hosted by pushshift.io.

B.2 End-to-end Training

Algorithm 3 Permute

Input: Adjacency matrix $\mathbf{A} \in \mathbb{R}^{N \times N}$; Node embeddings $\mathbf{X} \in \mathbb{R}^{N \times d}$; Node labels $\mathbf{Y} \in \mathbb{R}^{N \times d_y}$; Permutation $\pi \in \mathbb{R}^{N \times N}$;

1. $\mathbf{A}' \leftarrow \pi \cdot \mathbf{A} \cdot \pi^\top$
 2. $\mathbf{X}' \leftarrow \pi \cdot \mathbf{X}$
 2. $\mathbf{Y}' \leftarrow \pi \cdot \mathbf{Y}$
- Return $\mathbf{A}', \mathbf{X}', \mathbf{Y}'$
-

Algorithm 3 performs a permutation operation on the graph and node features based on the given permutation matrix and returns the permuted node features, labels and adjacency matrix.

Algorithm 4 Propagate

Input: Adjacency matrix $\mathbf{A} \in \mathbb{R}^{N \times N}$; Node embeddings $\mathbf{X} \in \mathbb{R}^{N \times d}$;

1. $\hat{\mathbf{A}} = \text{Normalized } \mathbf{A}$
 2. $\mathbf{X}' = \hat{\mathbf{A}}\mathbf{X}$
 3. Return $[\mathbf{X}, \mathbf{X}']$
-

The algorithm 4 outlines the Local Propagation Block (LCB), which plays a key role in the process. The LCB starts by aggregating neighborhood embeddings, optionally a normalization can be applied. Normalized \mathbf{A} can be derived in different ways. The standard GCN derives it as follows: $\hat{\mathbf{A}} = \mathbf{D}^{-1/2} \mathbf{A} \mathbf{D}^{-1/2}$, where $\mathbf{D}^{-1/2}$ where $\mathbf{D} = \text{diag}(\mathbf{A}\mathbf{1})$, and $\mathbf{1}$ is a column vector of ones. Preserving the original node features after propagation is essential. While some models, like GCN, achieve this by introducing self-edges to the original graph, this approach has a limitation: nodes treat their own embeddings and their neighbors' embeddings equally in terms of importance. To overcome this limitation, we adopt a different strategy. We concatenate the original node embeddings with the propagated embeddings, similar to a dense residual connection [74]. Notably, this step does not involve any learnable parameters. In Section 4.3, we explore several other variants with GNN models.

Algorithm 5 Projection

Input: Node embeddings $\mathbf{X} \in \mathbb{R}^{N \times d}$;

1. In parallel across N : $Z = \text{Linear}(X)$, $\text{Linear} : \mathcal{R}^d \rightarrow \mathcal{R}^{(K+1)d}$
 3. Reshape and split Z into X_1, X_2, \dots, X_K, V , where $X_k, V \in \mathcal{R}^{d \times N}$
- Return X_1, X_2, \dots, X_K, V
-

Algorithm 7 Forward pass of GECO

Input: Adjacency matrix $\mathbf{A} \in \mathbb{R}^{N \times N}$; Node embeddings $\mathbf{X} \in \mathbb{R}^{N \times d}$;

1. $\mathbf{X} = \text{BatchNorm}(\text{Propagate}(\mathbf{X}, \mathbf{A}))$
 2. $\mathbf{X} = \text{GCB}(\mathbf{X}, \mathbf{A})$
- Return \mathbf{X}
-

C Hyena Details

Equation 3 can be also expressed as $y_t = Tu$, where $T \in \mathbb{R}^{N \times N}$ is Toeplitz kernel matrix induced by filter z . Then the second-order Hyena operator with input $x \in \mathbb{R}^{N \times 1}$ defined as follows:

$$y = \text{Hyena}(x_1, x_2)x_3, \quad \text{Hyena}(x_1, x_2) = D_{x_2}TD_{x_1} \quad (7)$$

where x_1, x_2 , and x_3 are all projections of the input x , and $T \in \mathbb{R}^{N \times N}$ is used as a learnable convolution filter. In this context, T is learned by a neural network, where $T_{uv} = z_{u-v} = z_t = \gamma_\theta(t)$. $D_{x_1}, D_{x_2} \in \mathbb{R}^{N \times N}$ are diagonal matrices with x_1 and x_2 on their diagonals respectively.

Connection to Attention. Hyena(x_1, x_2) acts similar to attention matrix at Equation 2, however, it is realized by interleaving global convolutions and element-wise gating. Furthermore, $y = \text{Hyena}(x_1, x_2)x_3$ is efficiently computed without materializing the full matrix, using FFT convolutions and gating. Please refer to [19] for more details.

D Proofs

D.1 Decomposition of the Surrogate Attention Matrix

Let q, k and v be the linear projections of the input. Moreover, for simplicity, assume A is the surrogate attention matrix. [19] demonstrates that one can decompose the linear map $y = A_\varphi^\psi(q, k)v$ into a sequence of factors each dependent on a projection of the input such that $A_\varphi^\psi(q, k)v = A^\psi(q)A_\varphi(k)$. In this context, it is assumed that $D_q, D_k \in \mathbb{R}^{N \times N}$ are diagonal matrices with q and k are the respective entries in their main diagonal respectively. Then, we can have the following:

$$\begin{aligned} A^\psi(q) &= D_q S_\psi \\ A_\varphi(k) &= D_k S_\varphi \end{aligned} \quad (8)$$

Above, S_ψ and S_φ are Toeplitz matrices and are used as global convolution kernels with respective impulse responses. Moreover, the surrogate attention matrix is decomposed into two terms, $A^\psi(q)$ and $A_\varphi(k)$ which are computed by multiplying the diagonal matrices with the Toeplitz matrices:

$$A_\varphi^\psi(q, k)v = D_q S_\psi D_k S_\varphi \quad (9)$$

In the context of Hyena, the selection of ψ and φ matrices is chosen to be lower triangular, a choice well-suited for tasks involving causal language processing. In their publicly available repository⁶, the authors also explore a bi-directional variant. However, in this particular usage scenario, the kernel sizes are doubled to ensure proper input padding. This results in the convolution kernel’s length being twice that of the input, causing the weights to wrap around the input. This bi-directional convolution, while having bidirectional properties, is still fundamentally directional.

For our specific use case in graph applications, we configure the filter length to match the input length, corresponding to the number of nodes. Furthermore, we ensure that the Toeplitz matrices are designed with circular symmetry, thereby ensuring a non-causal convolution. In simpler terms, this means that any two nodes can mutually influence each other, as information from the future (a node with a higher node ID) can affect the past (a node with a lower node ID). Consequently, we represent S_ψ and S_φ as matrices with circular Toeplitz symmetry:

$$S_\psi = \begin{bmatrix} \psi_0 & \psi_{N-1} & \cdots & \psi_2 & \psi_1 \\ \psi_1 & \psi_0 & \cdots & \vdots & \vdots \\ \vdots & \ddots & \ddots & \psi_0 & \psi_{N-1} \\ \psi_{N-1} & \psi_{N-2} & \cdots & \psi_1 & \psi_0 \end{bmatrix}, \quad S_\varphi = \begin{bmatrix} \varphi_0 & \varphi_{N-1} & \cdots & \varphi_2 & \varphi_1 \\ \varphi_1 & \varphi_0 & \cdots & \vdots & \vdots \\ \vdots & \ddots & \ddots & \varphi_0 & \varphi_{N-1} \\ \varphi_{N-1} & \varphi_{N-2} & \cdots & \varphi_1 & \varphi_0 \end{bmatrix}. \quad (10)$$

Moreover, one can extend the Equation (9) as the following using the symmetric filters:

⁶<https://github.com/HazyResearch/safari>

$$\begin{aligned}
& \begin{bmatrix} q_0 & & & & & \\ & q_1 & & & & \\ & & \ddots & & & \\ & & & q_{N-2} & & \\ & & & & q_{N-1} & \end{bmatrix} \begin{bmatrix} \psi_0 & \psi_{N-1} & \cdots & \psi_2 & \psi_1 \\ \psi_1 & \psi_0 & \cdots & \vdots & \vdots \\ \vdots & \ddots & \ddots & \psi_0 & \psi_{N-1} \\ \psi_{N-1} & \psi_{N-2} & \cdots & \psi_1 & \psi_0 \end{bmatrix} \begin{bmatrix} k_0 & & & & \\ & k_1 & & & \\ & & \ddots & & \\ & & & k_{N-2} & \\ & & & & k_{N-1} \end{bmatrix} \begin{bmatrix} \varphi_0 & \varphi_{N-1} & \cdots & \varphi_2 & \varphi_1 \\ \varphi_1 & \varphi_0 & \cdots & \vdots & \vdots \\ \vdots & \ddots & \ddots & \varphi_0 & \varphi_{N-1} \\ \varphi_{N-1} & \varphi_{N-2} & \cdots & \varphi_1 & \varphi_0 \end{bmatrix} \\
& = \begin{bmatrix} q_0\psi_0 & q_0\psi_{N-1} & \cdots & q_0\psi_2 & q_0\psi_1 \\ q_1\psi_1 & q_1\psi_0 & \cdots & \vdots & \vdots \\ \vdots & \ddots & \ddots & q_{N-2}\psi_0 & q_{N-2}\psi_{N-1} \\ q_{N-1}\psi_{N-1} & q_{N-1}\psi_{N-2} & \cdots & q_{N-1}\psi_1 & q_{N-1}\psi_0 \end{bmatrix} \begin{bmatrix} k_0\varphi_0 & k_0\varphi_{N-1} & \cdots & k_0\varphi_2 & k_0\varphi_1 \\ k_1\varphi_1 & k_1\varphi_0 & \cdots & \vdots & \vdots \\ \vdots & \ddots & \ddots & k_{N-2}\varphi_0 & k_{N-2}\varphi_{N-1} \\ k_{N-1}\varphi_{N-1} & k_{N-1}\varphi_{N-2} & \cdots & k_{N-1}\varphi_1 & k_{N-1}\varphi_0 \end{bmatrix} \\
& \quad \quad \quad A_\psi(q) \quad \quad \quad A_\varphi(k)
\end{aligned} \tag{11}$$

Then, we can write the surrogate attention scores as:

$$A_\varphi^\psi(q, k)_{ij} = q_i \sum_{n=0}^{N-1} k_n \psi_{(i-n) \bmod N} \varphi_{(n-j) \bmod N} \tag{12}$$

D.2 Dynamic Random Permutation Sampling

The Janossy pooling function \bar{f} is a framework for constructing permutation-invariant functions from permutation-sensitive ones, such as RNNs, CNNs, LSTMs. In our case, we use it for global convolution models. In the original work [49], it is formally defined as:

Definition D.1 (Janossy Pooling [49]). Consider a function $\bar{f} : \mathbb{N} \times \mathbb{H}^\cup \times \mathbb{R}^b \rightarrow \mathbb{F}$ on variable-length but finite sequences \mathbf{h} , parameterized by $\theta^{(f)} \in \mathbb{R}^b$, $b > 0$. A permutation-invariant function $\bar{f} : \mathbb{N} \times \mathbb{H}^\cup \times \mathbb{R}^b \rightarrow \mathbb{F}$ is the Janossy function associated with \bar{f} if

$$\bar{f}(|\mathbf{h}|, \mathbf{h}; \theta^{(f)}) = \frac{1}{|\mathbf{h}|!} \sum_{\pi \in \Pi_{|\mathbf{h}|}} \bar{f}(|\mathbf{h}|, \mathbf{h}_\pi; \theta^{(f)}), \tag{13}$$

where $\Pi_{|\mathbf{h}|}$ is the set of all permutations, and \mathbf{h}_π is a particular permutation of the sequence.

The output of \bar{f} can further be chained with another neural network parameterized by $\theta^{(\rho)}$ [49]:

$$\bar{y}(\mathbf{x}; \theta^{(\rho)}, \theta^{(f)}, \theta^{(h)}) = \rho \left(\frac{1}{|\mathbf{h}|!} \sum_{\pi \in \Pi_{|\mathbf{h}|}} \bar{f}(|\mathbf{h}|, \mathbf{h}_\pi; \theta^{(f)}); \theta^{(\rho)} \right), \text{ where } \mathbf{h} \equiv h(\mathbf{x}; \theta^{(h)}). \tag{14}$$

However, notice that $\Pi_{|\mathbf{h}|}$ becomes computationally intractable for large graphs. To address this, [49] proposes the π -SGD, a stochastic optimization procedure that approximates the original objective by randomly sampling input permutations during training. Formally, π -SGD optimizes the modified objective \bar{J} :

$$\begin{aligned}
\bar{J}(\mathcal{D}; \theta^{(\rho)}, \theta^{(f)}, \theta^{(h)}) &= \frac{1}{N} \sum_{i=1}^N E_{\mathbf{s}_i} \left[L \left(\mathbf{y}^{(i)}, \rho \left(\bar{f}(|\mathbf{h}^{(i)}|, \mathbf{h}_{\mathbf{s}_i}^{(i)}; \theta^{(f)}); \theta^{(\rho)} \right) \right) \right] \\
&= \frac{1}{N} \sum_{i=1}^N \frac{1}{|\mathbf{h}^{(i)}|!} \sum_{\pi \in \mathbb{P}_{i|\mathbf{h}^{(i)}|}} L \left(\mathbf{y}^{(i)}, \rho \left(\bar{f}(|\mathbf{h}^{(i)}|, \mathbf{h}_\pi^{(i)}; \theta^{(f)}); \theta^{(\rho)} \right) \right).
\end{aligned} \tag{15}$$

where at iteration t , the parameters θ_t are updated as:

$$\theta_t = \theta_{t-1} - \eta_t \mathbf{Z}_t, \tag{16}$$

where \mathbf{Z}_t is the random gradient computed over a mini-batch \mathcal{B} by sampling random permutations $\mathbf{s}_i \sim \text{Uniform}(\Pi_{|\mathbf{h}^{(i)}|})$.

As demonstrated in [49], \bar{J} is permutation-invariant. If the function class modeling \bar{f} has sufficient expressive capacity to represent permutation-invariant functions, then minimizing \bar{J} will also minimize the original objective \bar{L} . Furthermore, minimizing \bar{J} implicitly regularizes \bar{f} to learn permutation-insensitive functions.

Proposition D.2 (π -SGD Convergence). *Under similar conditions as standard stochastic gradient descent (SGD), the π -SGD algorithm defined in Equation 16 enjoys properties of almost sure convergence to the optimal θ minimizing \bar{J} in Equation 15, as proven in [49].*

Effectively, π -SGD is an instance of Robbins-Monro stochastic approximation of gradient descent that optimizes \bar{J} by sampling random permutations of the input data during model training [49].

Note that these proofs are based on the original work [49]. For further details and complete proofs, please refer to the original work.

E Computational Complexity Discussion

Model	GNN	Dense GT	Layer GT	GraphGPS	GECO
Long-range Modeling	×	✓	×	✓	✓
Time	$\mathcal{O}(L(N+M))$	$\mathcal{O}(LN^2)$	$\mathcal{O}(L(N+M)+L^2)$	$\mathcal{O}(LN^2)$	$\mathcal{O}(L(N \log N + M))$
Memory	$\mathcal{O}(L(N+M))$	$\mathcal{O}(LN^2)$	$\mathcal{O}(L(N+M))$	$\mathcal{O}(LN^2)$	$\mathcal{O}(L(N \log N + M))$

Table 9: Computational Complexity Comparison for Full Batch Training

Table 9 presents an overview of the complexities associated with various models. It is important to note that while we provide specific categorizations, certain models within those categories may exhibit different complexities. Hence, the complexities presented here represent the general case.

E.1 Related Work

GNN models [3, 20] can be evaluated efficiently using sparse matrix operations in linear time with the number of nodes and edges in the graph. Although, some other models such as Graph Attention Networks (GAT) [21] and its variant GATv2 [22] which we categorize under *Sparse GT* at Section 2.2 has higher complexity, due to the attention mechanism. Asymptotically, these models can achieve higher computational efficiency compared to other methods such as Dense GT and Layer GT. Furthermore, they encompass a rapidly expanding line of research that investigates mini-batch sampling methods on GNNs [20, 75, 72, 66, 76].

Dense GT [10, 25, 11, 62, 26] involves pairwise attention between every node regardless of the connectivity of the graph, and hence has quadratic complexity with the number of nodes $\mathcal{O}(N^2)$. Recently, a variant of DenseGT called Relational Attention has been introduced, which involves additional edge updates, further increasing the overall complexity to $\mathcal{O}(N^3)$. Given that standard mini-batching methods cannot be applied to DenseGT, its application is limited to small datasets.

Layer GT. We categorize NAGphormer [23] under this category. NAGphormer employs attention on the layer (hop) tokens and exhibits a complexity similar to GNNs, given that the number of layers is typically fixed and smaller compared to the number of nodes or edges. As discussed in detail in Section G.7, while NAGphormer may not completely address issues inherited in GNNs, it offers several highly desirable properties. Firstly, it performs feature propagation as a preprocessing step, enabling the results to be reused. Additionally, during training, NAGphormer does not require consideration of the connectivity, which allows it to leverage off-the-shelf traditional mini-batch training methods, thereby achieving parallelism and scalability on large datasets.

Hybrid GT includes recently proposed GraphGPS framework [29]. GraphGPS combines the output of a GNN Module and Attention Module, and outputs of the two module is summed up within each layer. We discuss the differences between GECO and GraphGPS in detailed in Appendix G.6. The complexity of GraphGPS primarily depends on its attention module, which acts as a bottleneck. Despite offering subquadratic alternatives for attention, the reported results indicate that the best performance is consistently achieved when using the Transformer as the attention module. Consequently,

similar to Dense GT, GraphGPS exhibits a complexity of $\mathcal{O}(N^2)$, making it less suitable for large datasets. In essence, GraphGPS serves as a versatile framework for combining GNN and attention, along with their respective alternatives.

Positional Encodings (PE) play a crucial role for Graph Transformers. GT [10] incorporates Laplacian eigen-vectors (LE) as positional encodings (PE) to enrich node features with graph information. SAN [25] introduces learnable LE through permutation-invariant aggregation. Graphormer [11] uses node degrees as PE and shortest path distances as relative PE, achieving remarkable success in molecular benchmarks. GraphiT [62] proposes relative PE based on diffusion kernels. SAT [26] extracts substructures centered at nodes as additional tokens, while [27] uses substructure-based local attention with substructure tokens. GOAT [37] uses dimensionality reduction to reduce the computational cost of attention. [38] enhances attention with additional edge updates. While some PEs, like node degrees used in Graphormer [11], can be efficiently computed, others, such as Laplacian eigen vectors, Laplacian PE, or all pairs shortest path (for relative PE), involve computationally expensive operations, usually $\mathcal{O}(N^3)$ or higher. The good news is step can be computed once as a preprocessed step and does not necessarily be computed in GPU. Nevertheless, for extremely large graphs, computing PE can still be computationally infeasible.

E.2 GECO

GECO is composed of two building blocks: Local Propagation Block (LCB) and the Global Context Block (GCB). In Proposition 3.1, we discuss the complexity of LCB, which is $\mathcal{O}(N + M)$. This step exhibits a similar memory complexity of $\mathcal{O}(N + M)$.

E.3 End-to-End Training

Next, we analyze the complexity of GCB in Proposition 3.2, which is $\mathcal{O}(N \log N)$. In the paper, we specifically focus on the case when the GCB recurrence order is set to 2. However, we can generalize this to K recurrence, from which we derive the following complexity components:

1. Each GCB includes $(K + 1)$ linear projections, resulting in a complexity of $\mathcal{O}((K + 1)N)$.
2. Next, we have K element-wise gating operations, contributing a complexity of $\mathcal{O}(KN)$.
3. Finally, there are K FFT convolutions, where both the input and filter sizes are N , resulting in a complexity of $\mathcal{O}(KN \log N)$.

As a result, the generalized complexity of GCB can be expressed as $\mathcal{O}(KN \log N)$. Considering the end-to-end training complexity of GECO, we can combine the complexities of LCB and GCB, resulting in $\mathcal{O}(KN \log N + M)$.

Next, we examine the memory complexity of GECO, with a particular focus on the FFT convolutions used. The standard PyTorch [77] FFT Convolution typically requires $\mathcal{O}(N \log N)$ memory. However, it is possible to optimize this complexity to $\mathcal{O}(N)$ by leveraging fused kernel implementations of FFT Convolutions [44]. As a result, we can express GECO’s memory complexity as $\mathcal{O}(KN + M)$ when utilizing these fused FFT Convolution implementations, where K is the recurrence order.

F Experimental Details

F.1 Baselines

Our baselines through Tables 2 to 4 and 6 include GCN [3], Graphormer [11], GIN [22], GAT [21], GatedGCN [78, 16], PNA [79], DGN [80], CRaW1 [81], GIN-AK+ [82], SAN [25], SAT [26], EGT [83], GraphGPS [29], and Exphormer [31].

Our baselines for Table 4 include GCN [3], GraphSAGE [20], GraphSaint [72], ClusterGCN [84], GAT [21], JK-Net [59], GraphGPS [29] and Exphormer [31], Graphormer [11], SAN [25], SAT [26], ANS-GT [85], GraphGPS [29], HSGT [36].

F.2 Implementation and Compute Resources

Implementation. We have implemented our model using PyTorch-Geometric [86], GraphGPS [29] and Safari libraries [19]. For the evaluation at Section 4.1, we have integrated our code into the GraphGPS framework as a global attention module. For the evaluation at Section 4.2, we have implemented our own framework to efficiently run large datasets ⁷.

Compute Resources. We have conducted our experiments on an NVIDIA DGX Station A100 system with 4 80GB GPUs.

F.3 Hyperparameters

Baselines. For the baseline results presented at Tables 2 to 4 and 6 we reuse the results from GraphGPS and Exphormer [29, 31]. Moreover, for the baseline results presented at Table 4, we present the previously reported results in the literature [65, 31, 66, 36].

GECO. For datasets at Table 7, we drop in and replace the global attention module with GECO. The missing results are marked by $-$. Our choice of hyperparameters is guided by GraphGPS and Exphormer [29, 31]. We started with the hyperparameters recommended by the related work including optimizer configurations, positional encodings, and structural encodings. Then we proceed to hand-tune some optimizer configurations, dropout rates, and hidden dimensions by simple line search by taking validation results into account. On multiple datasets including PascalVOC, COCO, molpcha, and code2, we have eliminated the positional and structural encodings.

For datasets at Table 8, we have used hyperparameter optimization framework Optuna [87] with Tree-structured Parzen Estimator algorithm for hyperparameter suggestion with each tuning trial using a random seed. We reported the test accuracy achieved with the best validation configuration over 10 random seeds. As part of our public code release, we will provide all configuration files detailing our hyperparameter choices.

G Additional Experiments Discussions

G.1 Extended Runtime Study

Table 10: Runtime Comparison of GECO and FlashAttention [67] on synthetic datasets. $\mathcal{O}(N^2/(N \log N)) = \mathcal{O}(N/\log N)$ characterizes the speedup. Sparsity factor of each graph is set as $10/N$.

N	GECO (ms)	FlashAttention (ms)	Relative Speedup
512	1.88	0.27	0.14
1,024	2.13	0.32	0.15
2,048	2.11	0.31	0.15
4,096	2.42	0.32	0.13
8,192	2.12	0.51	0.24
16,384	2.13	1.84	0.86
32,768	2.63	6.92	2.63
65,536	3.73	28.74	7.70
131,072	6.21	115.23	18.56
262,144	15.74	458.64	29.14
524,288	41.72	1,830.29	43.87
1,048,576	83.90	7,317.04	87.21
2,097,152	173.15	29,305.77	169.25

In this subsection, we provide details on runtime ablation study in Section 4.3.

Experimental Setting. We have generated random graphs using Erdős-Rényi model. We increased the number of nodes from 512 to 4.2 million by doubling the number of nodes at consecutive points, using a total of 14 synthetic datasets. Furthermore, we set the sparsity factor of each graph to $10/N$, where N is the number of nodes as defined before, aligning the sparsity of the graph with that of large

⁷Our implementations will be open-sourced during or after the double-blind review process

node prediction datasets in Table 8. Additionally, we fixed the number of features at 108 across all datasets. We utilized publicly available FlashAttention implementation [67]⁸. For FlashAttention, we used 4 heads. In both GECO and FlashAttention, the number of hidden units is set as the number of features.

The results demonstrate that as the number of nodes grows larger, GECO achieves significant speedups with respect to FlashAttention. This is anticipated due to GECO’s complexity of $\mathcal{O}(N \log N + M)$, while attention’s complexity is $\mathcal{O}(N^2)$. Considering the sparsity of real-world datasets, N becomes a dominant factor, leading to a speedup characterized by $\mathcal{O}(N/\log N)$.

In summary, our findings support GECO’s efficiency for larger-scale applications, whereas for smaller scales, the choice between the two could be influenced by factors beyond just performance. As discussed throughout Section 1-Section 4, the scalability gains are not expected for small graphs. This is mostly due to low hardware utilization incurred by available FFT implementations. However, GECO still remains a promising approach due to its high prediction quality, as we demonstrated in Section 4.1. On the other hand, on larger graphs, GECO exhibits significant scalability, as demonstrated in Section 4.2. It consistently outperforms dense GTs on all large datasets and remains superior or competitive when compared to the orthogonal approaches.

G.2 PCQM4Mv2

Table 11: PCQM4Mv2 evaluation: the **first**, **second**, and **third** best are highlighted. *Validation* set is used for evaluation as *test* labels are private. We reuse results reported by [29].

Model	PCQM4Mv2			
	Test-dev MAE ↓	Validation MAE ↓	Training MAE ↓	# Param.
GCN	0.1398	0.1379	n/a	2.0M
GCN-virtual	0.1152	0.1153	n/a	4.9M
GIN	0.1218	0.1195	n/a	3.8M
GIN-virtual	0.1084	0.1083	n/a	6.7M
GRPE	0.0898	0.0890	n/a	46.2M
EGT	0.0872	0.0869	n/a	89.3M
Graphormer	n/a	0.0864	0.0348	48.3M
GPS-small	n/a	0.0938	0.0653	6.2M
GPS-medium	n/a	0.0858	0.0726	19.4M
GECO	n/a	0.08413	0.05782	6.2M

Due to space limitations, we have included only necessary information in Section 4.1 in Table 3. Appendix G.2 presents additional details.

G.3 Open Graph Benchmark Graph Level Tasks

As we wanted to focus on direct comparison between graph transformer models and due to space limitations, we have included only necessary information in Section 4.1 in Table 2. Appendix G.3 presents additional details. GECO still consistently secures top three when other GNN-based models are included. Some of these methods, such as CRaWl [81], incorporate features like random walk features that can be used in other approaches as well. In our comparison, we focus on evaluating GECO’s effectiveness with respect to attention or its alternatives.

G.4 Comparison with various Graph Transformers Variants

The survey [57] classifies existing methods for enhancing Transformer’s awareness of topological structures into three main categories: 1) Integrating GNNs as auxiliary modules (GA), (2) Enhancing positional embeddings from graphs (PE), and (3) Improving attention matrices using graphs (AT).

Regarding GA, the survey explores different approaches to combining off-the-shelf GNNs with Transformer. These methods involve adapting a series of GNNs and then applying a series of Transformers sequentially (before) [12], integrating GNNs and Transformers consecutively (Alternatively) [56], or utilizing them in parallel at each layer [29]. Notably, these models straightforwardly

⁸<https://github.com/Dao-AI/flash-attention>

Table 12: OGBG Eval.: the **first**, **second**, and **third** are highlighted. We reuse the results from [29].

Model	ogbg-molhiv	ogbg-molpcha	ogbg-ppa	ogbg-code2
	AUROC \uparrow	Avg. Precision \uparrow	Accuracy \uparrow	F1 score \uparrow
GCN+virtual node	0.7599 \pm 0.0119	0.2424 \pm 0.0034	0.6857 \pm 0.0061	0.1595 \pm 0.0018
GIN+virtual node	0.7707 \pm 0.0149	0.2703 \pm 0.0023	0.7037 \pm 0.0107	0.1581 \pm 0.0026
GatedGCN-LSPE	-	0.2670 \pm 0.0020	-	-
PNA	0.7905 \pm 0.0132	0.2838 \pm 0.0035	-	0.1570 \pm 0.0032
DeeperGCN	0.7858 \pm 0.0117	0.2781 \pm 0.0038	0.7712 \pm 0.0071	-
DGN	0.7970 \pm 0.0097	0.2885 \pm 0.0030	-	-
GSN (directional)	0.8039 \pm 0.0090	-	-	-
GSN (GIN+VN base)	0.7799 \pm 0.0100	-	-	-
CIN	0.8094 \pm 0.0057	-	-	-
GIN-AK+	0.7961 \pm 0.0119	0.2930 \pm 0.0044	-	-
CRaWI	-	0.2986 \pm 0.0025	-	-
ExpC	0.7799 \pm 0.0082	0.2342 \pm 0.0029	0.7976 \pm 0.0072	-
SAN	0.7785 \pm 0.2470	0.2765 \pm 0.0042	-	-
GraphTrans (GCN-Virtual)	-	0.2761 \pm 0.0029	-	0.1830 \pm 0.0024
K-Subtree SAT	-	-	0.7522 \pm 0.0056	0.1937 \pm 0.0028
GPS	0.7880 \pm 0.0101	0.2907 \pm 0.0028	0.8015 \pm 0.0033	0.1894 \pm 0.0024
GECO	0.7980 \pm 0.0200	0.2961 \pm 0.0008	0.7982 \pm 0.0042	0.1915 \pm 0.002

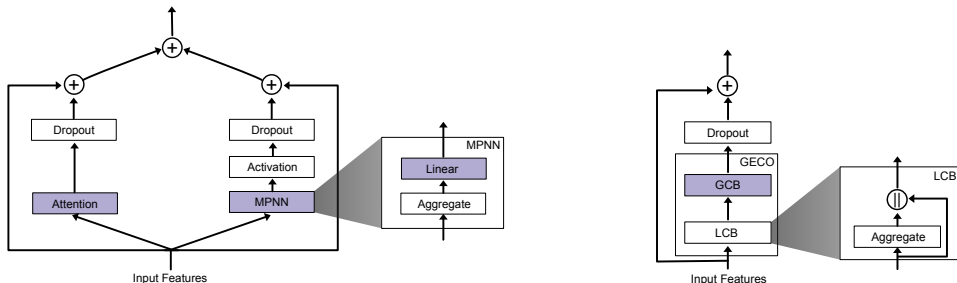
Table 13: Comparison with various Graph Methods from [57].

Model		molhiv	molpcha	Flickr	ogbn-arxiv
		ROC-AUC \uparrow	AP \uparrow	Acc \uparrow	Acc \uparrow
TF	vanilla	0.7466	0.1676	0.5279	0.5598
GA	before	0.7339	0.2269	0.5369	0.5614
	alter	0.7433	0.2474	0.5374	0.5599
	parallel	0.7750	0.2444	0.5379	0.5647
PE	degree	0.7506	0.1672	0.5291	0.5618
	eig	0.7407	0.2194	0.5278	0.5658
	svd	0.7350	0.1767	0.5317	0.5706
AT	SPB	0.7589	0.2621	0.5368	0.5605
	PMA	0.7314	0.2518	0.5288	0.5571
	Mask-1	0.7960	0.2662	0.5300	0.5598
	Mask-n	0.7423	0.2619	0.5359	0.5603
GECO (Ours)		0.7980 \pm 0.0200	0.2961 \pm 0.0008	0.5555 \pm 0.0025	0.7310 \pm 0.0024

merge pre-existing GNN and Transformer models, resulting in separate parameters and intermediate non-linearities for each module, with independently applied skip connections.

However, GECO does not precisely align with the taxonomy defined in the survey [57]. In GECO, we did not just use LCB as an auxiliary module to Transformer. Instead, we designed a new compact layer comprising local and global blocks. We eliminated the intermediate non-linearities and parameters to reduce the overall number of parameters, simplifying the training process. We applied skip connections to the entire GECO layer as a whole, rather than separately. These deliberate design choices distinguish GECO from the use of off-the-shelf methods. Please also refer to Appendix G.6 for further design details.

Furthermore, Table 13 highlight that GECO achieves consistent superior predictive quality across all datasets. Specifically, on arxiv and molpcha, GECO achieves significant relative improvements of up to 28.11% and 11.23%, respectively. We also note that, PE and AT are orthogonal approaches to our work.



(a) **GraphGPS Layer** consists of an MPNN and global attention modules with each module having its own skip connections and optional dropout. The modules are evaluated in parallel and summed up at the end. Both MPNN and attention modules usually have learnable weights.

(b) The **GECO Layer** comprises Local Propagation Block (LCB) and Global Context Block (GCB), evaluated sequentially with a skip connection across the entire block. Notably, LCB lacks learnable weights, serving as a pre-step to GCB, which incorporates the learnable weights.

Figure 3: A comparison between GraphGPS and GECO, where the layers with learnable weights are highlighted in color.

G.5 Comparison with Graph-ViT/MLP-Mixer

Table 14: Comparison of GECO with Graph-ViT and Graph-MLP-Mixer

Model	Peptides-func	Peptides-struct
	AP \uparrow	MAE \downarrow
Graph-MLP-Mixer	0.6970 ± 0.0080	0.2475 ± 0.0015
Graph-ViT	0.6942 ± 0.0075	0.2449 ± 0.0016
GECO	0.6975 ± 0.0025	0.2464 ± 0.0009

[32] proposed two models, namely Graph-ViT and Graph-MLP-Mixer that are generalization to popular ViT [33] and MLP-Mixer [34] architectures to graph structures focusing on graph-level tasks, such as those used in Section 4.1.

In Table 14, we summarize the results of GECO, Graph-ViT, and Graph-MLP-Mixer where results are available across all works. The results indicate that all models achieve competitive results and fall into each other’s confidence intervals, with GECO achieving a better mean of Peptides-func, Graph-ViT achieving a better mean on Peptides struct.

However Graph-ViT/MLP-Mixer only focuses on graph level tasks consisting of small number of average number, and their scalability to the large node prediction datasets has no evidence. This is likely because they require graph re-partitioning at every training epoch using METIS partitioner. While this approaches may be feasible for small graphs, it is very costly strategy for large node prediction datasets such as those in Section 4.2. On the other hand, our method does not require such partitioning; it can be simply used as a drop-in replacement for the self-attention of GTs.

G.6 Comparison with GraphGPS

As GECO can be considered a hybrid method, a natural question arises regarding what sets it apart from GraphGPS. In this section, we delve into the distinctions between these two models. The fundamental difference between GECO and GraphGPS layers lies in their design as illustrated in Figure 3. Given input features, the MPNN and attention modules of GraphGPS are evaluated in parallel and then summed up. Each module encompasses its own set of learnable weights, activation functions, dropout layers, and residual connections. On the other hand, in the case of GECO, LCB and GCB are evaluated sequentially. Notably, LCB does not incorporate any learnable weights, activation functions, or dropout layers; it functions as a feature propagation block with a dense skip connection. Instead, GECO’s weights are encapsulated within the GCB block. Furthermore, the residual connection is applied to the entire GECO block. In practice, GECO and GraphGPS can be combined in various ways. In our experiments, we chose to employ GECO as an attention module to

facilitate a direct comparison with GraphGPS and Exphormer. However, it is possible to integrate GraphGPS and GECO differently. Potential options also include substituting GCB with a Transformer or replacing LCB with an MPNN.

G.7 Connection between Jumping Knowledge Networks and NAGphormer

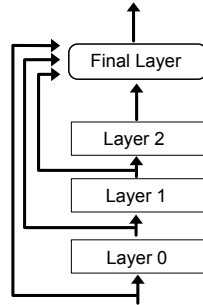


Figure 4: Illustration of JK-Nets with 3 layers. It is important to note that the Final Layer can be implemented using different layers, and it does not necessarily have to be the same as the intermediate layers. Although the original work While the original work [59] did not introduce a dense skip connection from the original inputs to the Final Layer, we have included it here for the sake of consistency in notation.

Jumping Knowledge Networks (JK-Nets) [59] have been introduced as GNNs with a variant of dense skip connection. The difference from the original dense skip connections [74] is that instead of establishing dense connections between every consecutive layer, JK-Nets establish dense skip connections from each layer to a final aggregation layer as illustrated in Figure 4. Given this framework, we can recover NAGphormer as a special case of JK-Nets with two simple configurations:

1. Replace non-linear transformation function of the GNN with the identity function. That is we do not use learnable weights, simply utilize traditional feature propagation.
2. Set Final-Layer as multi-head attention.

With these two simple modifications, one can recover the NAGphormer as a specific instance of JK-Nets. Here NAGphormer corresponds to an MHA layer with tokens produced by a GNN with no learnable weights, or traditional feature propagation.